universität wien

DIPLOMARBEIT / DIPLOMA THESIS

Titel der Diplomarbeit / Title of the Diploma Thesis

„Effects of GLUT1, LAT1, SGLT1/2 Inhibitors on the PET-Tracer Uptake in Multicellular Tumor Spheroids“

verfasst von / submitted by

Alexandra Schwarz

angestrebter akademischer Grad / in partial fulfilment of the requirements for the degree of

Magistra der Pharmazie (Mag.pharm.)

Wien, 2019 / Vienna, 2019

Studienkennzahl lt. Studienblatt / degree programme code as it appears on the student record sheet:	A 449
Studienrichtung lt. Studienblatt / degree programme as it appears on the student record sheet:	Diplomstudium Pharmazie
Betreut von / Supervisor:	o. Univ.-Prof. i. R. Mag. Dr. Helmut Viernstein

Acknowledgements

First of all, I would like to thank o. Univ.-Prof. Mag. Dr. Helmut Viernstein for giving me the opportunity to carry out my diploma thesis at the Department of Pharmaceutical Technology and Biopharmaceutics.

My sincere gratefulness goes to the head of the division of the Department of Nuclear Medicine Univ.-Prof. Dr. Markus Hacker, who gave access to the research facilities. In addition, I would like to express my thankfulness to Prof. Mag. Dr. Markus Mitterhauser, Prof. Mag. Dr. Wolfgang Wadsak, Mag. Dr. Lukas Nics and Mag.^{a} Dr.^{in} Cécile Philippe, who initiated the opportunity of being part of this team.

I would like to express my gratitude to my research advisor Mag.^{a} Dr.^{in} Verena Pichler, who always lent a helping hand and stood by my side whenever I needed advice. Because of you I have been able to gain more insight in the field of Nuclear Medicine. Thank you for your valuable guidance and patience.

Furthermore, I would like to express my special thanks to Mag.^{a} Theresa Balber for synthesizing [^{18}F]FET needed for my experiments. In addition, I would like to thank Dr.^{in} Chrysoula Vraka, Msc, Mag.^{a} Eva-Maria Klebermass, Neydher Berroteran-Infante, Msc and all the other members of the department. It was such a pleasure to work with all of you.

Last but not least, I would like to thank my loving and caring family, amazing friends and motivational colleagues for their unconditional support. Without your encouragement I never would have been able to achieve my goals.

Abstract

In industrialized countries, cancer is one of the leading causes of mortality. Consequently, there is a steady increase in research to develop new methods for effective cancer treatment. In order to succeed in cancer therapy, it is necessary to recognize and avoid limiting factors as decreased responsiveness to radiation and chemotherapeutics. This requires know-how about characteristics of tumor tissue, which is allowed by cultivation of multicellular tumor spheroids. Therefore, the use of multicellular tumor spheroids in the evaluation of anticancer drugs derives from their promising physiological simulation of tumor tissue, which cannot be obtained in 2D cell culture models. Furthermore, an increased application of multicellular tumor spheroids in the preclinical PET-tracer evaluation for cancer diagnosis would enable a more selective repertory of potential active agents and consequently the possibility of reducing animal experiments. Fortunately, prior examined PET-tracers allow for an evaluation of the application as well as adequacy of spheroids.

The aim of this diploma thesis was the observation of effects of different inhibitors (apigenin, BCH, phlorizin) on the accumulation of various PET-tracers ([^{18}F]FDG, [^{18}F]FEC, [^{18}F]FET, [^{11}C]MET) in cultivated multicellular tumor spheroids of different cell lines (HT-29, HCT-116, HT-1080). Therefore, spheroid cultivation took place in previously agarose coated 96-well plates, referring to adequate cultivation methods established for each cell line. Afterwards, four different concentrations of the inhibitor were applied. In order to determine the PET-tracer accumulation 3 MBq of the particular tracer were added to each spheroid and after incubation time was up, all samples were measured in the gamma counter.

In case of apigenin and phlorizin, results showed a reduction of accumulation of [^{18}F]FDG in all tested cell lines. However, BCH inhibited the accumulation only in cell line HCT-116 as well as in spheroids of cell line HT-29 in the highest concentration.
The accumulation of tracer [^{18}F]FEC was not significantly affected by BCH. Both apigenin as well as phlorizin showed a significant effect in tracer accumulation only at the highest concentration.

apigenin and phlorizin had a noticeably bigger impact on the [^{18}F]FET-accumulation compared to the inhibitor BCH.

In case of [^{11}C]MET, all inhibitors led to a reduction of accumulation in the tested cell lines.

Zusammenfassung

Tumorerkrankungen stellen nach koronaren Herzerkrankungen die häufigste Todesursache in der westlichen Welt dar. Dieser Fakt hat zur Folge, dass sich vor allem in den letzten Jahrzehnten die Suche nach Ansätzen, Tumorgewebe schnellst möglich gezielt behandeln zu können, großer Beliebtheit in der Forschung erfreut. Um jedoch eine erfolgreiche Krebstherapie garantieren zu können, ist es notwendig, limitierende Faktoren wie verminderte Ansprechbarkeit auf Bestrahlung oder Chemotherapeutika zu erkennen und zu umgehen. Dies setzt eine gute Kenntnis über die Charakteristika des Tumorgewebes voraus, welche mittels Kultivierung multizellulärer Tumor Sphäroide angestrebt werden kann. Deren Einsatz in der Evaluierung von Chemotherapeutika ist auf die vielversprechende physiologische Simulation von Tumorgewebe zurückzuführen, welche bei 2D Zellkulturmodellen zu wünschen übrig lässt. Weiters würde der vermehrte Einsatz von multizellulären Tumor Sphäroiden in der präklinischen PET-Tracer Evaluierung zur Diagnose von Tumoren eine gezieltere Selektion potentieller Wirkstoffe ermöglichen und in weiterer Folge zu einer verminderten Anzahl notwendiger Tierversuche beitragen. Mit Hilfe von bereits gut untersuchten PET-Tracern kann eine Beurteilung über die Anwendung und Eignung von Sphäroiden erfolgen.

Ziel dieser Diplomarbeit war nun die Beobachtung der Auswirkung verschiedenster Inhibitoren (Apigenin, BCH, Phlorizin) auf die Akkumulation verschiedenster PET-Tracer ([^{18}F]FDG, [^{18}F]FEC, [^{18}F]FET, [^{11}C]MET) in kultivierten multizellulären Tumor Sphäroide mehrerer Zelllinien (HT-29, HCT-116, HT-1080). Hierfür erfolgte die Kultivierung der Sphäroide in zuvor mit Agarose beschichteten 96-well Platten nach einer für jede Zell-linie bereits etablierten, geeigneten Methode. Anschließend fand die Hemmung mit einem Inhibitor in vier verschiedenen Konzentrationen statt. Um nun die PET-Tracer Akkumulation bestimmen zu können, wurde jedes Sphäroid mit 3 MBq des jeweiligen Tracers versehen und die Aufnahme nach Ende der Inkubationszeit im Gamma Counter vermessen.

Im Falle von Apigenin und Phlorizin zeigten die erhaltenen Ergebnisse eine Reduktion der [^{18}F]FDG-Akkumulation in allen getesteten Zelllinien. BCH hingehen hemmte die Tracer-

Akkumulation nur in der Zelllinie HCT-116 sowie in der höchsten Konzentration auch in Sphäroiden der Zelllinie HT-29.

Die Akkumulation des Tracers [^{18}F]FEC wurde durch den Inhibitor BCH nicht merklich beeinflusst. Sowohl Apigenin als auch Phlorizin zeigten nur bei der höchsten Konzentration einen signifikanten Effekt auf die Akkumulation.

Apigenin und Phlorizin hatten einen deutlich stärkeren Effekt auf die [^{18}F]FET-Akkumulation als der Inhibitor BCH.

Im Falle von [^{11}C]MET führten alle Inhibitoren zu einer Reduktion der Akkumulation in den getesteten Zelllinien.

TABLE OF CONTENT

1 Introduction

1.1 Multicellular tumor spheroids

1.1.1 Importance of multicellular tumor spheroids

A few decades ago, the basic principle of multicellular tumor spheroids, developed by Holtfreter, was adapted to cancer research and has since then essentially made a contribution to our knowledge of cellular reactions to both diagnostic and therapeutic interventions. [1] The term multicellular tumor spheroid describes self-assembled dense cell aggregates, characterized by close cell-cell interactions and serving as a 3D cell culture model, amongst which their cultivation is a successful approach to obtain the functionality of cancer cells in human beings, since 2D cell assays are limited in the reflection of *in vivo* cell and tissue characteristics. [2-7]

However, solid tumors are surrounded by stromal and close-by tumor cells as well as extracellular matrix components. In addition, environmental interactions like cell-cell interactions and local gradients of oxygen, nutrients and growth factors have an impact not to be underestimated on the cells' behavior and condition. By causing a cellular heterogeneity within the spheroid, 3D cell culture models outplay monolayer morphology. Furthermore, high density cell arrangement results in a penetration barrier for drugs and other metabolites. [2-6] All these characteristics led to the promising establishment of various sorts of *in vitro* methods, representing a helpful link between *in vitro* and *in vivo* studies. Nevertheless, spheroids are not surrounded by other human derived cells such as fibroblasts or endothelial cells and therefore cannot be fully equated with real tumors in human beings.

The aim of radiopharmaceutical research is the selection of the most promising candidates in drug development before taking it to expensive research stages like *in vivo* tumor modeling or even clinical trials. Since it is impossible to reflect the entire functional behavior of cells *in vivo* correctly by a monolayer morphology emerging from cells cultured in a flask, cultivation of multicellular tumor spheroids incorporates an improvement to do so. By embedding spheroids in hydrogels, like Matrigel or collagen, attempts are made to approach physiological states even more. [8]

1.1.2 Characteristics of multicellular tumor spheroids

Cells which are cultured in a flask are automatically forced into monolayer morphology and therefore lack cell-cell interactions as well as cell-matrix interactions, which might lead to a false positive response to chemotherapeutical agents during *in vitro* drug evaluation. Subsequently, same chemotherapeutical agents might show low efficiency in *in vivo* testing, whereas other agents were dismissed too soon from further studies. Furthermore, since 2D growth implies optimal exposure to oxygen and nutrients of the culture medium, the appearance of molecular gradients is not given. Because of these missing features, 2D cultures are not fully capable of reflecting the functional behavior of cells found *in vivo*. These facts emphasize the need of 3D cell culture models for efficient *in vitro* drug testing. However, multicellular tumor spheroids allow for a closer simulation of real tumor tissue. [6, 9-11]

When examining a spheroid under a microscope, different regions can be defined. Spheroids possess a developable rim of proliferating cells, representing the surface layer. Furthermore, an intermediate layer and a perinecrotic region, which is a layer of non-proliferating hypoxic cells surrounding a necrotic core, can be observed (figure 1). In spheroids reaching a diameter of more than 500 µm, a low amount of oxygen and nutrient exposure within the inner core leads to cell damage and subsequently necrosis. The main function of cells in the inner core consists of the prevention of cell damages by increasing expression of proteins necessary for energy production. In recent studies, McMahon *et al.* additionally analyzed the expression of proteins within different regions of spheroids and came to the conclusion that proteins correlated with cell death were upregulated in necrotic regions. [12-14]

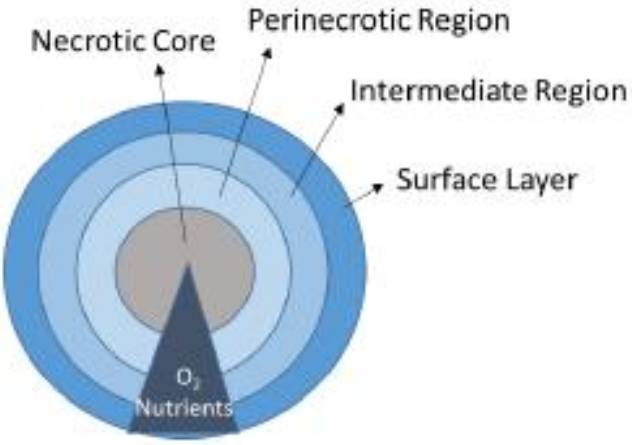

Figure 1: *Different regions observed in a multicellular tumor spheroid. (Source: Litos L. The evaluation of PET-tracer accumulation in multicellular tumor sphe-roids. 2017; page 4)*

Moreover, the growth kinetics observed in multicellular tumor spheroids approximate those in human tumors. Due to adequate supply of nutrients and oxygen a phase of exponential growth, followed by later retardation of cell growth, is shown. The consequence of limitations in glucose as well as oxygen resourcing results in an increase of non-proliferating cells within the spheroid, which has an impact on the growth behavior (figure 2). Hence, both necrotic and perinecrotic cells emit growth inhibiting factors, which leads to attenuation of surrounding cells of the intermediate and surface layer. [12, 15]

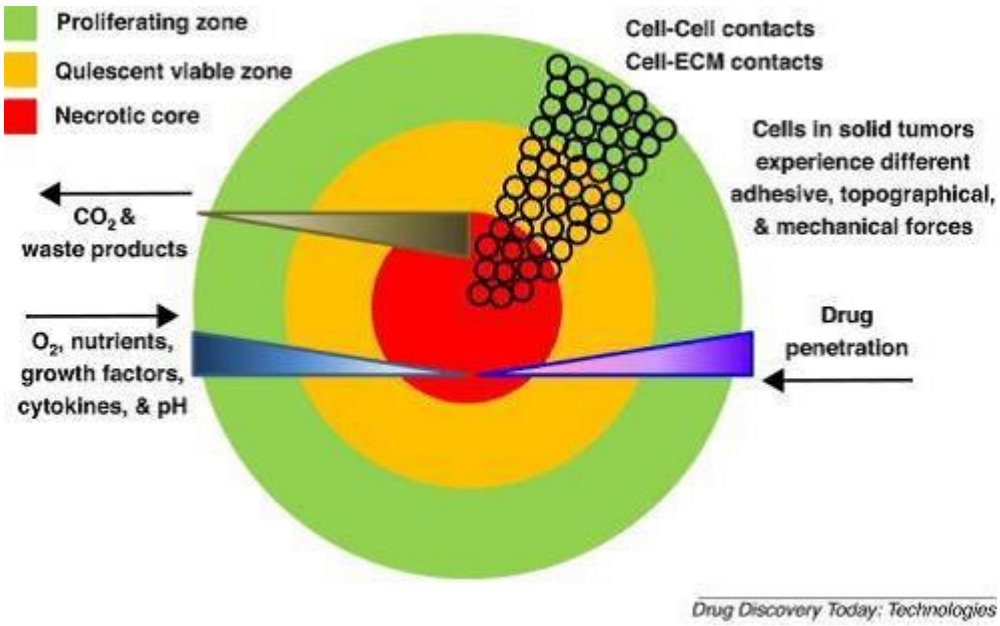

Figure 2: *Illustration of supply of nutrients and oxygen in a multicellular tumor spheroid. (Source: https://www.sciencedirect.com/science/article/abs/pii/S1740674917300112, downloaded on 25.01.2019)*

The consequence of tumor cells spreading into other healthy tissues results in damage of the extracellular matrix and subsequently in release of stored growth factors, which leads to three-dimensional organization of tumor cells, encouraging resistance to anti-cancer drugs. Last cannot be observed in tumor cells, which are cultivated in a bidimensional monolayer. A further advantage of three-dimensional cell arrangement is the interaction of cells with each other as well as with an extracellular matrix, which is also observed in tumor tissue. In tumors, the extracellular matrix serves as a depot for multiple growth factors and protects against drug-induced apoptosis. The importance of the cell-matrix connection is illustrated in the spheroid model, since apoptotic activities are mainly induced in the inner core, whose cells lack attachment to the extracellular matrix. Although this protective effect is important for the survival of healthy cells during chemotherapy, science faces a problem regarding efficiency in the process of killing tumor cells. [10, 11]

1.1.3 Application of multicellular tumor spheroids

When it comes to comparing 2D cell monolayers with multicellular tumor spheroids, last ones are more similar to *in vivo* tumors concerning their cellular heterogeneity and growth behavior. The fact that tumor tissue is often resistant to chemotherapeutical agents or ra-

diation derives from their ability of developing anti-apoptosis effects, which might be caused by hypoxic and necrotic regions as well as cell-matrix interactions. [16] Additionally, drug resistance is being reinforced by high density of tissue structure as well as the building of tight cell-cell interactions, which leads to a penetration barrier and therefore results in an alteration of drug metabolism. In 2D tumor cell monolayers, these kinds of characteristics cannot be observed, which makes obvious, why multicellular tumor spheroids are rather used for discovery of anti-cancer drugs. For evaluation of the response of multicellular tumor spheroids to chemotherapeutical agents, parameters like cell survival or spheroid growth delay are a matter of particular interest. With these and similar parameters as determined end points of research studies, unsuitable substances can be easily preselected conducting drug screenings, which offers a possibility to animal testing reduction. [6, 7, 17, 18]

A further application of multicellular tumor spheroids apart from drug discovery, are drug transport and uptake studies, which are important for PET-tracer evaluation. Although many uptake studies showed promising results that PET-screenings could be used for treatment monitoring of various cancers, further data of PET-tracers accumulation in spheroids is still required. Despite the similar characteristics of multicellular tumor spheroids compared with physiological tumors, they cannot be completely equalized with real tumor tissue, which are surrounded by fibroblasts or endothelial cells. In order to attempt resemblance with physiological conditions, spheroids are embedded in hydrogels, for example collagen. To obtain even better mimicry, attempts of investigating the effects of chemotherapeutical agents in the presence of physiological immune cells like natural killer cells, macrophages, lymphocytes or T-cells were carried out by co-culturing them with multicellular tumor spheroids. This method could lead to development of new immunotherapeutic strategies. [6, 19] In conclusion, as demonstrated above, both sole multicellular tumor spheroid cultivation as well as spheroid co-culture models by far have more potential than their use in the field of cancer research only.

1.1.4 Imaging of multicellular tumor spheroids

In research, cell-based assays are an indispensable tool. Because of the three-dimensional cell arrangement of spheroids, imaging is more of a challenge compared to 2D cell monolayers. However, for observing spheroid growth behavior and formation, a conventional bright field microscopy can be applied. In order to gain more specific infor-

mation on a spheroid's interior as well as visualization of necrotic regions within the aggregate, fluorescence based assays and staining with conventional dies are approved methods. [7]

1.1.5 Generation of multicellular tumor spheroids

A fundamental benefit of multicellular tumor spheroids cultivation is the practicability in every standard cell culture laboratory without the need of any special equipment. Generally, it can be distinguished between scaffold based methods and tumor spheroid building without the addition of scaffold building agents. The techniques used for spheroid formation are based on cell aggregate building obtained through gravitational as well as rotational forces. There are various ways to cultivate spheroids including the spinner culture method or the hanging-drop-method, whereas a disadvantage of these techniques is the noticeable difference in shape and size of the spheroids. Therefore, an advanced pellet culture system was developed in order to achieve uniformity of yielded spheroids by coating 96-well plates and creating an ultra-low attachment surface.

1.2 Tumor imaging *via* PET

Tumor related pathologies are one of the leading causes of mortality worldwide, which underlines the importance of early diagnosis as well as continuous therapy monitoring in order to increase the chance of cure. The advantage of the non-invasive positron emission tomography (PET) in comparison to other established imaging techniques like computer tomography (CT) is featured by providing information about a body's metabolic events. Hence, PET is perfectly suited for early diagnosis as well as monitoring therapy progress during radiation therapy. Nevertheless, modern PET-scanners are usually combined with magnetic resonance imaging (MRI) or computer tomography in order to assemble both physiological and anatomical information.

Radiopharmaceuticals consist of a vehicle molecule which should provide a high degree of specificity and selectivity. They are linked to a positron emitting radionuclide. The molecule structure determines the pharmacokinetics within the organism, like distribution or metabolism of the tracer. However, the isotope is responsible for a detectable signal for visualization. The functionality of PET-imaging is based on a radiotracer's capability of emitting a

positron from its nucleus. These injected tracers are radiolabeled molecules whose positron collides with an electron which subsequently leads to their annihilation followed by emission of two 510 keV gamma-rays in opposite directions (figure 3). Those rays are detected by a photomultiplier which further allows images to be reconstructed, showing the distribution and concentration of the applied tracer within the human body. [20]

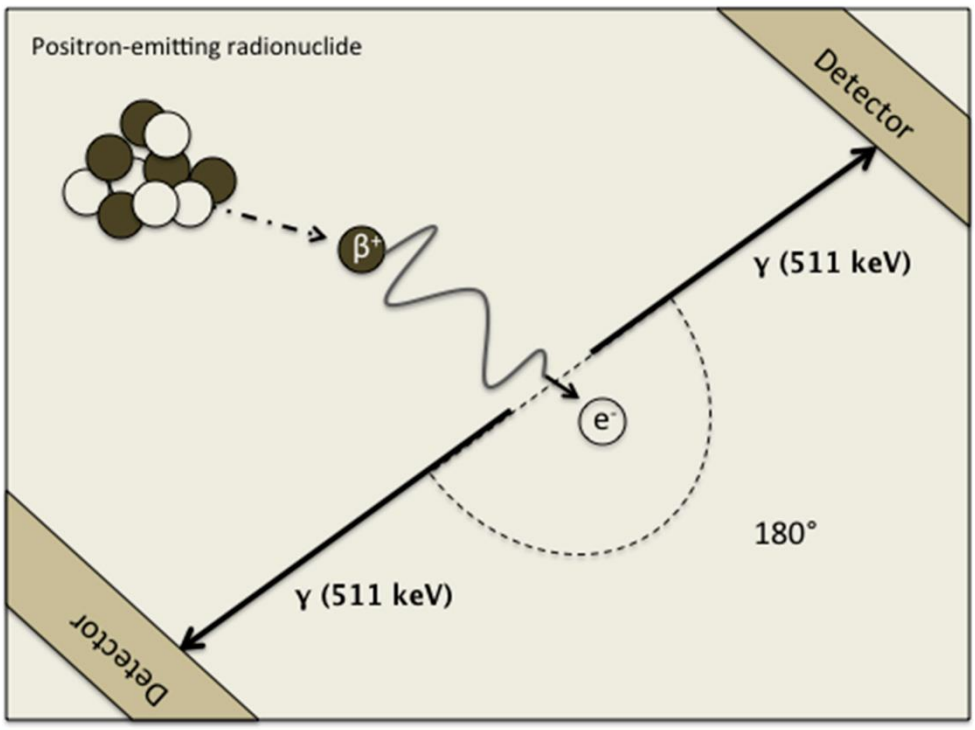

Figure 3: *Illustration of the principle of positron emitting tomography.*
(Source: https://www.mdpi.com/1010-660X/54/3/47, downloaded on 27.01.2019)

Most frequently used radionuclides like fluorine-18, carbon-11and nitrogen-13 can be produced in a cyclotron, whereas gallium-68 is usually obtained with a generator. Typical characteristics of these isotopes are their relatively short half-lives, like 20 min for carbon-11 or 110 min for fluorine-18. They are incorporated into so-called parent molecules, which either bind to specific receptors or are metabolized as their unlabeled counterpart by the body.

In this thesis the following tracers were analysed: [^{18}F]fluorodeoxyglucose ([^{18}F]FDG), [^{18}F]fluoroethyl-L-tyrosine ([^{18}F]FET), [^{18}F]fluoroethylcholine ([^{18}F]FEC) and [^{11}C]methionine ([^{11}C]MET), whereupon the glucose analogue [^{18}F]FDG is the most frequently used one in oncology PET-scans worldwide.

1.3 Glucose transporters and their upregulation in cancer cells

Most cancer cells demonstrate increased glucose uptake as well as increased dependence on glucose for cell growth and as a source of energy, while healthy cells utilize amino acids, lipids and glucose in a more balanced way. Increased glucose uptake in cancer is achieved primarily by upregulation of glucose transporters, so called GLUTs. GLUT1 is a basic glucose transporter expressed in almost all cell types – abundant in brain and erythrocytes (figure 4). Its level of overexpression in almost all types of cancer is correlated with grade, proliferation and differentiation in various cancers and can be used as hypoxic marker in malignant tumors. Clinical studies also have shown that high levels of GLUT1 expression come along with poor survival prognosis. (21)

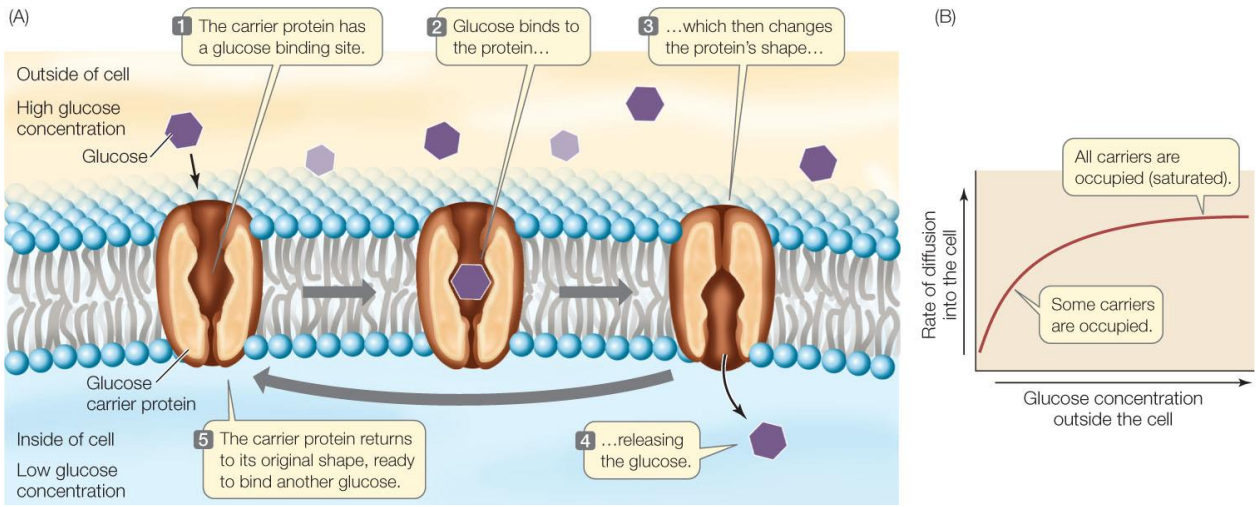

Figure 4: *(A) Transport of a glucose molecule by a carrier protein adapting its shape (B) This graph displays the correlation between glucose concentration outside the cell and its diffusion into the cell.*
(Source:http://www.macmillanhighered.com/BrainHoney/Resource/6716/digital_first_content/trunk/test/hillis2e/asset/img_ch5/c05_fig06.html, downloaded on 25.02.2019)

1.4 Anticancer therapeutics targeting glucose transporters

By taking advantage of an improved understanding of the altered cancer metabolism compared to that of normal cells, numerous anticancer therapeutics have been developed successfully in order to target proteins and enzymes involved in glucose transport and metabolism. The rapid proliferation and growth of cancer cells require changes in glucose transport, which is drastically upregulated in most cancers. This change in glucose metab-

olism of cancer cellsis termed the Warburg effect. In addition, GLUTs enhance survival and drug resistance of cancer cells, which leads to the conclusion of them being a good target for therapeutic intervention and therefore one of the major focuses of this new research area.

However, there are also some disadvantages associated with the strategy of inhibiting GLUTs. First of all, glucose transporters are not only expressed by cancer, but also by healthy cells, which inevitably leads to GLUT inhibition in these cells. That is why it is absolutely essential to identify a therapeutic window in behalf of this anticancer strategy's success. Fortunately, a human's body's key organs such as the brain and heart can use ketone bodies as a substitute for glucose in order to keep up their functionality. Nevertheless, the outcome of GLUT inhibition should not lead to a significant energy loss for these vital organs. Additionally, cancer cells' reliance on glucose is not absolute. Moreover, it has been hypothesized that targeting a pathway such as glucose metabolism rather than a specific protein or enzyme may be more effective. This awareness is based on the observation that most cancer cells somehow can always bypass the aspired inhibition of a target drug by shifting from glucose metabolism to a compensatory pathway like glutamine metabolism. In order to shut down a cancer cell's metabolism more effectively, glutamine metabolism as a target for anti-cancer drugs used together with GLUT inhibition could be a possible way to achieve cancer cell death. [21] Nevertheless, these approaches need to be tested more precisely in the future.

1.5 Mechanisms of inhibition

Basically, it can be distinguished between three main types of transporter inhibition mechanisms – competitive inhibition, non-competitive inhibition and uncompetitive inhibition (figure 5).

Competitive inhibition is the simplest form of inhibition. Due to structure similarity of substrate and inhibitor both compete with similar affinity for the binding site of the transporter. Whereas the receptor might be unable to metabolize an inhibitor, a substrate is normally processed to a product or different metabolite in order to increase its water solubility. However, high substrate concentrations can be added to overcome the inhibitory effects, which results in an increase of the Michaelis-Menten constant Km.

In contrast, non-competitive inhibition describes the inhibitor binding to the allosteric site, which is distant from the active site. Binding the allosteric site subsequently results in change of the conformation of the active site, which makes substrate binding and product formation less likely.

One of the rarest forms of inhibition is the uncompetitive inhibition. In this case, binding of the inhibitor only occurs in presence of an already existing complex of receptor and substrate. Moreover, the substrate itself might act as an inhibitor, if appearing in excess. [22]

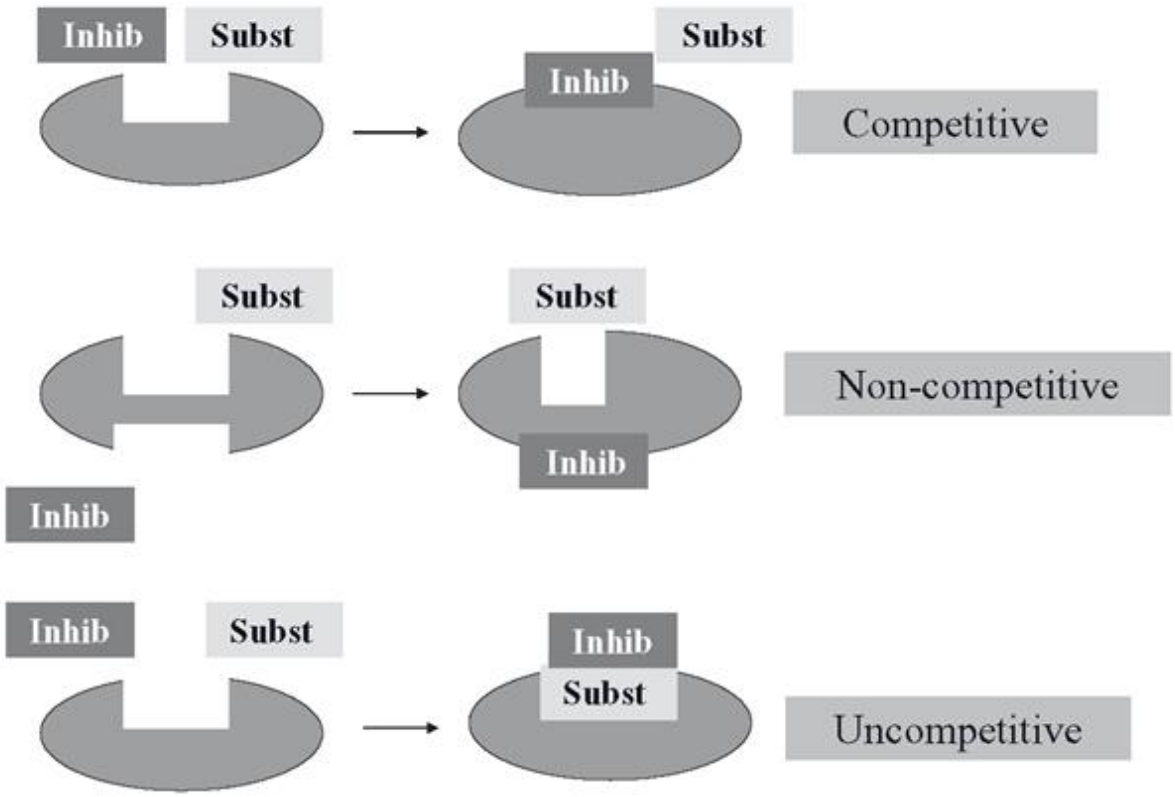

Figure 5: *Illustration of competitive, non-competitive and uncompetitive inhibition of receptors. (Source: http://what-when-how.com/human-drug-metabolism/mechanisms-of-inhibition-cytochrome-p450-inhibition-human-drug-metabolism-part-1/, downloaded on 15.02.2019)*

1.6 Types of transport mechanisms

Since inhibition or induction of membrane transporters may result in an alteration of pharmacokinetics and pharmacodynamics of various compounds, transporters are now considered as critical regulators of drug disposition, therapeutic efficacy and adverse drug reactions. Several well characterized cell lines over-expressing transporters are used to

study their role in regards of intracellular drug accumulation. [23] Although transporters and channels, existing of several helical transmembrane domains connected by intracellular and extracellular loops, have shown complex multiphasic transport kinetics observed in multicellular organisms they are structurally and functionally distinctive. However, recent studies showed that some transporters are likely to show characteristics similar to channels and vice versa. As transport kinetics may result from the coexistence of multiple transport systems allowing the uptake of one substance, identification and functional characterization of a channel or a transporter is not that simple. [24]

Intracellular accumulation of small molecular-weight compounds is conducted by two major processes, simple passive diffusion through the phospholipid membrane on the one hand or by membrane transporters or channels on the other hand, depending on the properties of the cell and the structural characteristics of the compound. The plasma membrane itself serves as a selective barrier between the cell and its environment whose maintenance of integrity is of supreme importance for homeostasis and cell survival. Membranes consist of a phospholipid bilayer with intercalated agile proteins. [23]

In terms of intracellular drug transport by passive diffusion the lipophilicity of the transported molecule, the molecular mass and the number of hydrogen bond donors and acceptors play a major role in entering a cell. Moreover, passive drug diffusion operates concentration independent and therefore is non-saturable and not affected by inhibition of membrane proteins. [23] Simple diffusion normally occurs with small and non-polar solutes such as oxygen and carbon dioxide, whereas facilitated diffusion, which can be subclassified in channel or carrier mediated diffusion, applies to substances that are small charged or polar solutes. However, they can pass in and out of a cell with the assistance of plasma membrane proteins. Channel mediated diffusion describes the movement of an ion through a water filled protein channel which possess a selective gated pore formed by specific residues of protein, which is mostly specific to one type of ion. It can be distinguished between a leak channel, which is continuously open and a gated channel, opening due to a stimulus. Carrier mediated diffusion involves the movement of small polar molecules such as simple sugars or carbohydrates and amino acids across the membrane by actually changing their shape during this process. In order to be accessible either intracellularly or extracellularly a substrate induces a conformational change that consequently

triggers an alteration from substrate binding with high affinity on one side to low-affinity substrate binding and release on the other side of the membrane. [24]

The main difference between passive and active transport is that former goes with the concentration gradient and therefore does not require energy, whereas for active transport a source of free energy is needed, as is the movement of solute against a concentration gradient, provided either by hydrolysis of ATP or by coupling with an energetically beneficial flow, where two substances are moved in the same direction (symport) or counter-flow (antiport) of ions. [24] Membrane trafficking mechanisms are dictated by the constant flux of proteins and lipids to and from intracellular organelles to the surface of the cell by vesicles which are cellular organelles composed of a lipid bilayer. Exocytosis is the process by which cytoplasmic organelles fuse with the plasma membrane in order to secret materials from the cell to the interstitial fluid outside of the cell, whereas endocytosis mediates the internalization and accumulation of drug metabolites in subcellular compartments. [23]

ATP binding cassette transporters (ABC) and solute carriers (SLC) are two major types involved in the transport of endogenous molecules such as amino acids, carbohydrates, inorganic ions as well as a wide range of therapeutic drugs. These transporters are highly expressed in the kidney, liver, intestine and endothelial barriers. The family of SLC transporters are membrane proteins predominantly involved in the uptake of substrates into cells and can act as uniporters, symporters or antiporters, but do not rely directly on ATP hydrolysis. In contrast, ABC drug transporters require ATP as source of energy and regulate the efflux across the plasma membrane of various drugs and their metabolites. Importantly, many of the substrates of ABC drug transporters overlap with those handled by SLC transporters. Also, two co-administered molecules can have an overlapping affinity for a single transporter, contributing to interactions between those drugs. [23]

1.7 Inhibitors used in multicellular tumor spheroids

1.7.1 GLUT1 inhibitor apigenin

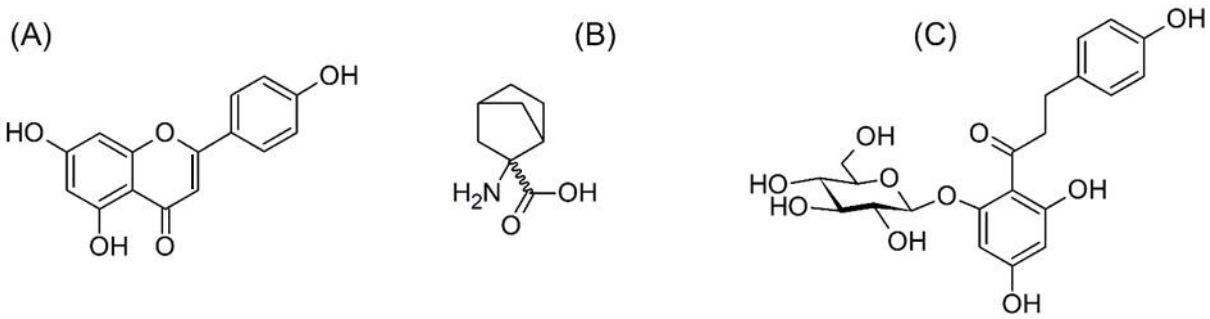

Figure 6: *Structures of the inhibitory compounds (a) apigenin (API), (b) 2-amino-2-norbornanecarboxylic acid (BCH), and (c) phlorizin (PLZ)*

Apigenin is a widely distributed plant-derived flavonoid compound existing abundantly in common fruits and vegetables (figure 6A). The substance (IUPAC name: 5,7-dihydroxy-2-(4-hydroxyphenyl)chromen-4-one) with the molecular formula $C_{15}H_{10}O_5$ has a molecular weight of 270.24 g/mol. Previous studies have already reported apigenin's potential biological effects such as anti-mutagenic, anti-oxidant, anti-cancer, and anti-inflammatory activities. Furthermore, various studies have pointed out its inhibition effects towards several drug transporters in human cancer cells. It was demonstrated that the flavonoid is able to inhibit glucose uptake and downregulate the expression of GLUT1 (SLC2A1) at both the levels of transcription and translation. Moreover, this occurrence is linked to downregulation of the PI3K/Akt pathway, whose increased activity is often implicated in resistance to cancer therapeutics. [25-28]

1.7.2 LAT1 inhibitor BCH

In drug development in human cancers, LAT1 (SLC7A5) is one of the most actively studied amino acid transporters and plays a critical role in matters of one's overexpression. LAT is a large neutral amino acid antiporter which provides (cancer) cells with amino acids as leucine, isoleucine, valine, phenylalanine, tyrosine, tryptophan and methionine for protein synthesis (figure 7). It is Na^+-independent, which explains the relatively low transport capacity of this transporter. Recent studies have shown contribution to tumor cell proliferation, angiogenesis, and survival of various human neoplasms of highly expressed LAT1.

Therefore, a significant overexpression indeed is a factor indicating a bad prognosis in various human cancers.

The activity of CD98 in the heterodimeric complex LAT1/CD98 has been investigated for years and led to the demonstration, that LAT1 is the only transport responsible unit, able to mediate antiport of amino acids with the same properties of the heterodimer, while CD98 does not exhibit any function in regards of transport. Nevertheless, its importance is predicated on trafficking LAT1 to its definitive location in plasma membrane. [29,30]

Critical residues of the substrate binding site not freely accessible by molecules other than substrate as well as for gating of LAT1 have been probed in many studies. In conclusion, residues F252, S342, C335 are involved in substrate recognition, whereas C407 plays a role in substrate binding from the internal side. Inhibitors exhibiting the most potent effects react with C407 *via* disulphide bond. However, recognition of an inhibitor could also be ascribed to their substrate resembling structure. Taken together, F252 revealed to be a gate opening element of LAT1, allowing substrate entry in the translocation site. Furthermore, the other residues S342 and C335 are responsible of substrate docking on the external side of the protein. This knowledge also leads to the assumption, that presence of substrate does not prohibit an interaction between an inhibitor and LAT1. [29, 30]

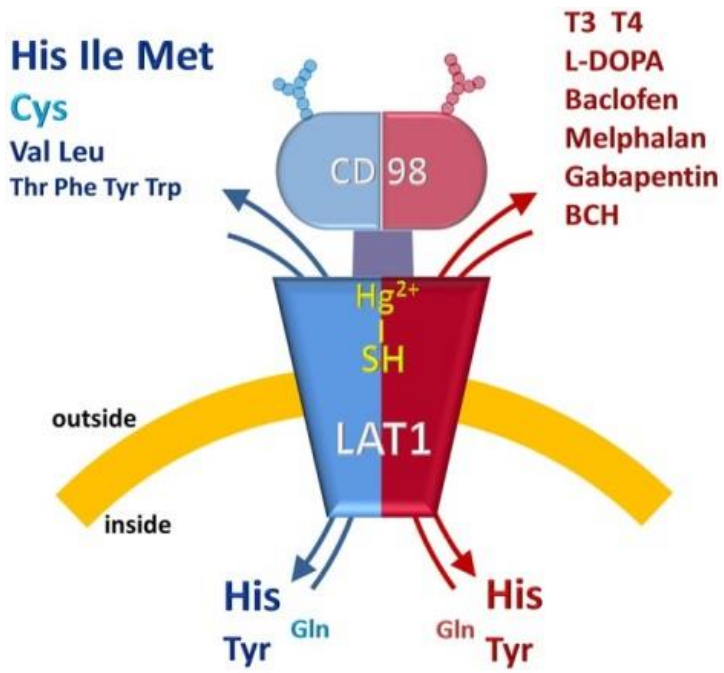

Figure 7: *Representation of the heterodimeric complex LAT1/CD98 and its specificity towards amino acids colored in blue as well as towards non-amino acid substrates like hormones, drugs*

and inhibitors such as BCH colored in red.
(Source: https://www.frontiersin.org/articles/10.3389/fchem.2018.00243/full , downloaded on 15.02.2019)

BCH (figure 6B), also known as 3-aminobicyclo[2.2.1]heptane-3-carboxylic acid with a molecular weight of 155.19 g/mol and the molecular formula $C_8H_{13}NO_2$ is an inhibitor of the L-type amino acid transporter 1 (LAT1). It can block all four isoforms of the LAT family: L-type amino acid transporter 1 (LAT1), LAT2, LAT3, and LAT4. According to a study, BCH inhibited L-leucine transport in a concentration-dependent manner as well as cell growth in a time-dependent manner. [33] Moreover, high concentration of BCH is needed for inhibition of highly proliferous cancer cells. Furthermore, it was shown that inhibition with BCH is a slowly reversible process, as it was possible to detach BCH from the cell surface. In addition to inhibiting the uptake of neutral amino acids, BCH suppresses a specific signal pathway that leads to DNA synthesis and cell proliferation. However, known LAT1 inhibitors' weakness is their lack of selectivity over other transporters. [31-37]

1.7.3 SGLT1/2 inhibitor phlorizin

The dihydrochalcone and naturally occurring phenol glycoside phlorizin (figure 6C) belongs to the group of flavonoids and was isolated from an apple tree's bark for the first time in 1835. Because of its dual SGLT1/2 inhibitory activity, phlorizin has served as lead compound in the development of new drugs achieving both activities. Moreover, other flavonoids enriched in plant extracts besides phlorizin (1-[2,4-dihydroxy-6-[(2S,3R,4S,5S,6R)-3,4,5-trihydroxy-6-(hydroxymethyl)oxan-2-yl]oxyphenyl]-3-(4-hydroxyphenyl)propan-1-one) have been investigated with regard to their potency of reducing postprandial blood glucose levels, which can be helpful in the prevention or even supplementary treatment of type 2 diabetes. [38-41] As mentioned above, phlorizin is a reversible, competitive inhibitor of sodium-glucose co-transporters SGLT1 and SGLT2 – which can be found in the intestine and kidney, respectively – as it competes with D-glucose for binding to the carrier (figure 8). SGLT1/2 inhibitors' main pharmacological activity is predicated on the reabsorption of filtered glucose from the primary urine and was attributed with the ability of reducing renal glucose transport by increasing glucose excretion in the kidneys, which consequently results in lower blood glucose. This process occurs at two main sites, whereas the proximal tubule accounts for 90% of reabsorption through SGLT2 (SLC5A2) and remaining 10%

through SGLT1 (SLC5A1). By using sodium gradients created by Na^+/K^+-ATPase pumps at the basolateral border of the cell membranes, SGLT transports sodium and glucose into the interstitium. Shortly after, glucose is passively transported by GLUT2 along its concentration gradient into the cell. Hence, it was observed that phlorizin binds to the outside of SGLT at two domains, one representing the sugar binding site on the one hand and a glucose binding site on the other hand. This double interaction emphasizes the high affinity of the compound in comparison to D-glucose. [42]

Phlorizin could have been a potential agent in the treatment of type 2 diabetes. Unfortunately, its therapeutic potential is limited by its poor oral bioavailability accompanied by its tendency to be hydrolysed by enterobacteria to its aglycone phloretin. Additionally, gastrointestinal adverse events after oral application of phlorizin can be explained by its lack of specificity for SGLT2 and rather actions on SGLT1, managing the intestinal glucose absorption by endothelial cells. Therefore, it has been excelled by more selective and promising synthetic SGLT2 inhibiting analogues like dapagliflozin, empagliflozin and canagliflozin which have been approved for treatment of type 2 diabetes. [38-41]

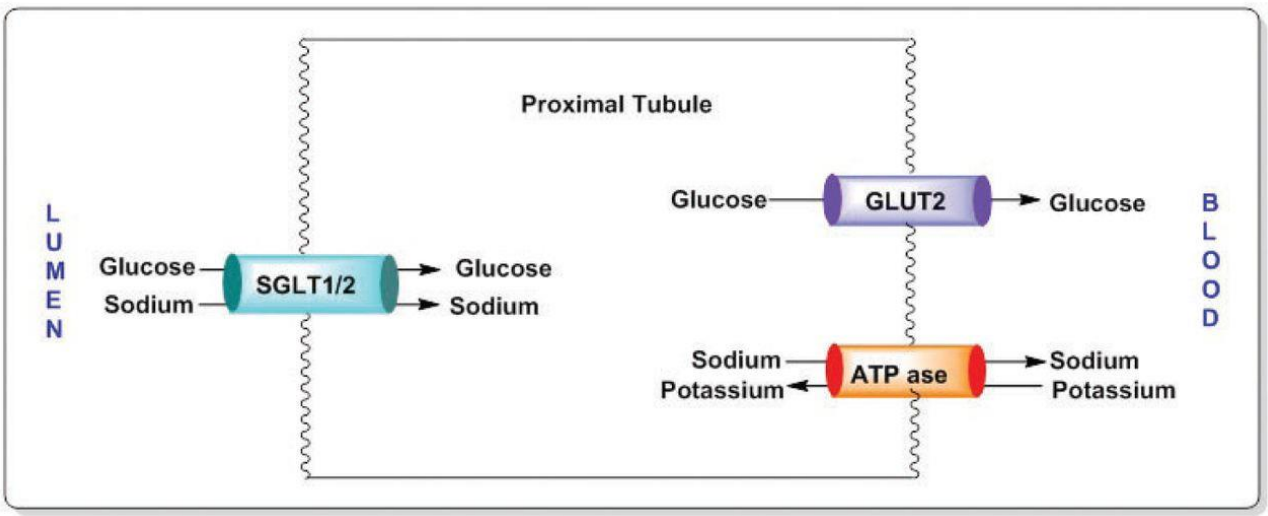

Figure 8: *SGLT1/2 use energy created by the Na^+/K^+-ATPase pump to transport glucose across the apical membrane. These co-transporters are an example of secondary active transport as they operate against the glucose gradient.*
(Source: http://spectrum.diabetesjournals.org/content/30/2/137, downloaded on 16.02.2019)

1.8 PET-Tracers used in multicellular tumor spheroids

1.8.1 [^{18}F]FDG

[^{18}F]FDG is – just like glucose – recognized by the GLUT-transporters which actively transport it into cells, where an enzyme called hexokinase phosphorylates it to FDG-6-phosphate. Since FDG lacks a hydroxyl group in the second position compared to glucose, [^{18}F]FDG is not available for further glycolysis and FDG-6-phosphate gets trapped within the cell. Mostly, pathologically high mitotic rates as in cancerous cells go along with alterations in glucose metabolism, which leads to a higher expression of glucose transporters as well as an up-regulated hexokinase activity. Caused by the fact that all cells metabolize glucose, [^{18}F]FDG is not specific for tumor cells. Nevertheless, its accumulation within tumor tissue is increased. Therefore, it is inevitable letting the patient fast for 4 to 6 hours before PET-scan is performed. (20, 43, 44)

1.8.2 [^{18}F]FEC

Choline is a quaternary ammonium compound used for phospholipid synthesis in cell membranes and transmembrane signaling. It is incorporated into cells *via* the choline transporter, which is dependent from adenosine-triphosphate, and then phosphorylated to phosphocholine by the enzyme choline kinase. Major mechanisms of phosphocholine accumulation in tumor cells are the malignancy-induced upregulation of the enzyme including enhancement of the choline transport, subsequent phosphorylation and activation of phosphatidylcholine specific phospholipases, whose membrane choline is an essential part of. In conclusion, labelled choline derivatives as [^{18}F]FEC are trapped in form of phosphatidylcholine in the membrane of a prostate's tumor cells and its metastases. (45)

1.8.3 [^{18}F]FET

For the last decade, positron emission tomography with the tracer [^{18}F]fluoroethyltyrosine has been used in the evaluation of patients with mainly brain tumors, showing significant accumulation. The ^{18}F-radiolabelled amino acid outplays [^{11}C]MET in regards of its much longer half-life of approximately 110 minutes. It also is superior to [^{18}F]FDG in points of

biopsy guidance and treatment procedure of cerebral gliomas. Hence, amino acids like [^{18}F]FET are the preferred tracers for the clinical management of brain tumors. [46-48]

1.8.4 [^{11}C]MET

Positron emission tomography with [^{11}C]MET provides information about amino acid metabolism in brain tumors. The disadvantage of this tracer is its very short half-life of approximately 20 minutes due to the carbon isotope. Therefore, [^{18}F]FET was developed as a longer-living alternative to [^{11}C]methionine and additionally is suitable to distinguish between inflammation and residual tumor tissue.

1.9 Sample measurement with a gamma counter

A gamma counter is a standard tool for measuring radioactivity of single samples which are placed on purpose-built vials and moved along a track automatically. Its operating mode is used in research and development of radioactive compounds which could be utilized for diagnosis and treatment of diseases. In principle, a gamma counter quantifies the gamma radiation emitted by a radionuclide. Depending on the half-life of the analyzed isotope, measurement times may vary from a few seconds to several hours. The scintillation crystal, which interacts with gamma rays, surrounds the radioactive sample. As soon as the rays are absorbed, flashes of light are produced, which is called scintillation. Subsequently, a photomultiplier converts the light into electrical currents, making it possible to draw conclusions from the energy of the radiation. On the one hand, it could be possible that light of interacting photons may never be detected, if their energy is too low and therefore absorbed in the scintillation crystal. On the other hand, photons might just pass right through the crystal without interaction, if the energy is too high. Therefore, the thickness of the crystal also matters when it comes to detecting rays. [49]

2 Aim

A major drawback in current preclinical evaluation is that 2D cell culture often not match the *in vivo* situation, due to lack of simulation of physiological tumor tissue characteristics. Therefore, *in vitro* testing of chemotherapeutical efficiency in multicellular tumor spheroids enjoyed great popularity in the last decades. However, this 3D model is not very common for the investigation of diagnostic agents. Due to the similarity of these multicellular tumor spheroids to malign lesions of the human body concerning morphology and functional features, spheroids represent a growing field to cover the span between 2D cell monolayers and the *in vivo* situation. Hence, the use of multicellular tumor spheroids significantly contributes to reduction of the number of small animals needed for *in vivo* experiments and therefore significantly comply with the 3R's (reduce, refine, replace) of animal testing.

The major aim of this diploma thesis was the evaluation of influences of inhibitors of the GLUT1, SGLT1/2 and LAT1 on the accumulation of four different PET-tracer in multicellular tumor spheroids.

For this purpose accumulation experiments were performed, using [^{18}F]FDG, [^{18}F]FET, [^{18}F]FEC and [^{11}C]MET as PET-tracers. The use of especially carbon-11 and fluorine-18 as radioactive isotopes was highly challenging in terms of available time of the experiments due to the relatively low half-life. Multicellular tumor spheroids were grown by cultivating fibrosarcoma cell line HT-1080, colon carcinoma cell line HCT-116 and human colorectal adenocarcinoma cell line HT-29. With intent to impact the accumulation mechanism of the multicellular tumor spheroids', SGLT1/2 inhibitor phlorizin, LAT1 inhibitor BCH and GLUT1 inhibitor apigenin were applied.

3 Materials and Methods

3.1 Cell lines and culture conditions

To create multicellular tumor spheroids human colorectal adenocarcinoma cell line HT-29, fibrosarcoma cell line HT-1080 and colon carcinoma cell line HCT-116 were used. All cell lines were cultivated in 25 cm² cell culture flasks (Cellstar®, Greiner Bio-One, Frickenhausen, Germany) and stored at 37°C in a cell incubator under humidified atmosphere containing 5% CO_2.

For cell line HT-29, RPMI medium, supplemented with 10% fetal bovine serum (FBS) and 1% L-glutamine that prevents degradation and ammonia building in both adherent and suspension cultures was used. Both HCT-116 and HT-1080 cells were nourished with MEM medium, which was also supplemented with the same amount of FBS and L-glutamine. All cell culture media and supplements were purchased from Gibco™ (Thermo Scientific, Massachusetts, United States).

Approximately every two to three days cell culture media was exchanged to provide the cells with fresh nutrients. All routine maintenance procedures were performed under sterile conditions by using a laminar air flow hood.

3.1.1 Splitting cells

In order to avoid dying cells they needed to be split when they reached a confluency of approximately 80-90% according to standard protocol. The flasks were checked daily under a microscope to determine the current confluency. First of all, old medium was removed and cells were washed with 5 mL Gibco® Dulbecco's phosphate buffered saline (DPBS). Afterwards, 500 µL of Accutase® solution (Sigma Aldrich, Missouri, United States) was added, followed by incubating the flask for 5 to 10 minutes at 37°C in order to completely detach all cells from the ground of the flask. Afterwards, the cells were resuspended in 1 mL of complete growth medium containing FBS to stop the Accutase® reaction. Then an aliquot of the suspension was pipetted in a new flask in order to count the cells and perform cell seeding. 5 mL supplemented growth medium were added to the rest of the suspension.

3.1.2 Counting cells

Whenever new spheroids were needed to be seeded it was necessary to determine the cell count of the suspension. Therefore, an aliquot of the desired cell suspension which was produced in course of the splitting procedure was used. 20 µL of the resuspended solution were taken up and slowly pipetted at the edge of the cover glass of a Neubauer hemocytometer until the area was covered. The suspension was drawn inside the hemocytometer by capillary action. Afterwards, cells were counted according to instructions in four big squares using a microscope with magnification. Then, the average of squares counted was calculated, which amounts the cells per mL when multiplied by 1×10^4.

3.1.3 Thawing cells

For thawing prior frozen cells in Nunc® CryoTubes® a water bath was used. In the meantime a centrifuge tube containing 5 mL of medium was prepared. As soon as there was only a little piece of frozen medium left, the tube was disinfected and put in the laminar air flow. The whole content was transferred quickly to the tube containing the medium to be resuspended. Afterwards, the cells were centrifuged for 3 to 5 min at 1200 rpm. Then supernatant was removed and only the pellet was resuspended in 1 mL medium. Finally, the suspension was transferred to a labelled flask containing 8 to 10 mL of medium and incubated at 37°C in a humidified atmosphere. The medium was changed the next day in order to get rid of potential residues of DMSO as well as dead cells. After approximately one and a half week cells behaved normally again regarding proliferation and adhesion and could be used for further experiments.

3.1.4 Freezing cells

In advance of freezing the requested cells, Nunc® CryoTubes® were labeled and Mr. Frosty™ (Thermo Scientific, Massachusetts, United States), a freezing container used to achieve the optimal rate of cooling close to 1°C/min for cell preservation, was put in the fridge. For preparing the freezing medium 10% DMSO were added to avoid crystal formation. After cell splitting was performed as outlined above, cells were centrifuged for 5 minutes at 1200 rpm, the pellet was resuspended in freezing medium. Then, cell suspension was aliquoted into the tubes at a volume of 1 mL each. Eventually, the tubes were put

in the Mr. Frosty™ and stored at -80°C. For long-time storage, cell suspensions were stored in liquid nitrogen.

3.1.5 Agarose coating of 96-well plates

To be able to form multicellular spheroids, 96-well plates were coated with 1.5% agarose gel to create a low attachment surface. For the gel preparation 675 mg low gelling temperature agarose (Sigma Aldrich, Missouri, United States) was weighed in a weighing boat and transferred to a 50 mL Falcon™ tube under sterile conditions. Afterwards, the closed tube was exposed to UV light for at least 30 min to sterilize the agarose. Then, the agarose was suspended in 44.3 mL sterile water and the suspension was heated in a water bath for 1 h at approximately 70-80°C. It was important to shake the flask from time to time to make sure that the agarose completely dissolves. After that the tube with agarose was stored in a beaker with hot water to prevent solidification of the gel. For coating, approximately 10 mL of the warm solution were poured in a sterile Petri dish under laminar air flow. A 100 µL multichannel pipette (Eppendorf, Hamburg, Germany) was used to fill a row of wells of a 96-well plate and immediately suck up the liquid again. At this step it was important to remove the agarose gel completely without any bubbles inside of the well. Now the agarose solution was dispensed in the reservoir and the next row was continues to be coated. When the agarose solution in the reservoir started to solidify the reservoir was exchanged and filled with fresh agarose solution to avoid the formation of air bubbles. Finally, the coated plates were stored in a fridge at 4°C at least overnight to make sure that the gel has solidified. Long-time storage also takes place in the fridge.

3.2 Formation of multicellular tumor spheroids

To achieve the formation of spheroids, cells were detached from the flask by using Accutase® as described in the splitting protocol above and counted with a Neubauer hemocytometer. Depending on the cell lines, different cell concentrations per well were determined. In case of cell line HT-29 spheroid, seeding with an initial cell concentration of 500 cells per well was implemented and for HCT-116 as well as HT-1080 3000 cells per well were chosen.

The outlining rows of pre-coated 96-well plates were filled with 100 µL Gibco® Dulbecco's phosphate buffered saline (DPBS) to avoid evaporation of cell medium. Cell suspensions were diluted with the respective growth media to the desired cell count in tilted petri dishes to ease pipetting procedure. Afterwards a multichannel pipette (Eppendorf, Hamburg, Germany) was used to place 100 µL of each cell suspension into the wells of the agarose coated 96-well plate. Then, the plates were incubated and not moved at 37°C under humidified atmosphere with 5% CO_2 for three days. This rest period was necessary to guarantee a steady formation of the multicellular tumor spheroids. In order to determine their diameter, spheroids were monitored regularly using an Olympus IMT-2 microscope, equipped with a XC50 camera connected to a computer running Cell^B software. After reaching a diameter of approximately 500 µm, the spheroids were available for further experiments.

Similar results can be obtained by using the hanging-drop-method. In this case, small drops of cell suspensions are placed on the bottom of a Petri dish's inverted cover plate, which is then placed on the dish. Consequently, cells start to build aggregates by slowly settling to the bottom of the drop. The most time-consuming step consists in transfer of the aggregates to 96-well plates in order to enable further spheroid growth.

3.3 Cell viability assay – live and dead staining

For visualization of necrotic and proliferating regions within multicellular tumor spheroids calcein acetoxymethylester (Sigma Aldrich, Missouri, United States), a fluorescent dye with emission wavelengths of 517 nm was used for staining of the living cells (green fluorescence) and propidium iodide (Sigma Aldrich, Missouri, United States), a red-fluorescent nuclear and chromosome counterstain with emission wavelengths of 617 nm, marked only dead cells. To begin with, the cultivated spheroids with the desired diameter were transferred to flat bottomed 96-well plates in triplicates to avoid measurement error due to curvature of round 96-well plates. Afterwards, spheroids were washed twice with DPBS after the media was removed without damaging the spheroids. In the next step, cells were incubated with 100 µL of propidium iodide (diluted 1:500 in growth medium) for 6 hours at 37°C. For the last 15 minutes of incubation time 100 µL of calcein AM (diluted 1:400 in nutrient solution) were added. Afterwards, staining solutions were removed and spheroids

washed twice and finally covered with DPBS for examination under an Olympus IMT-2 fluorescence microscope equipped with a camera.

3.4 Alamar blue assay

The aim of the following Alamar blue assay was to find a suitable concentration of the inhibitor interacting with the receptor, but without inducing cell death, in order to avoid misleading results caused by necrotic or apoptotic cells.

Therefore, a stock solution containing a concentration of 2 mM was chosen to be started with. After weighing approximately 2 mg of substance in a Falcon^{TM} tube, the amount of substance n was calculated using a molecular weight of 472.44 g/mol, which led to volume of added growth media by mathematical conversion of the formula c=n/V. In order to increase dissolubility of phlorizin in growth media DMSO as organic modifier was added to the Falcon^{TM} tube and put in a water bath as well as shaken from time to time. At this step, it was crucial to ensure that the compound completely dissolved.

Then, the first ten wells of a 96-well plate were labelled with numbers from one to ten and subsequently filled with 500 µL of growth media each. To receive nine different concentrations of phlorizin starting at the highest of 1 mM down to 3.9 µM a serial dilution was performed. Well number ten was filled with growth media only as negative control (figure 9).

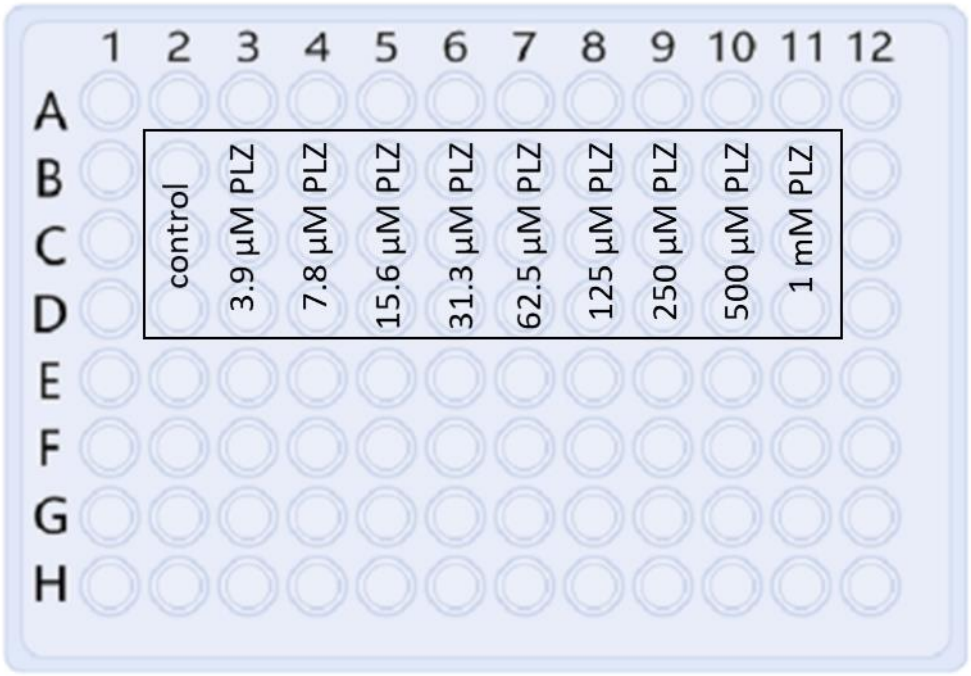

Figure 9: *The pattern of pipetting in order to obtain 9 different phlorizin concentrations as well as a control in triplicates*

As soon as the preparation of the different concentrations was accomplished, 100 µL of each concentration were pipetted in triplicates to previously selected spheroids of one cell line and incubated for 24 hours at 37°C under humidified atmosphere with 5% CO_2. The spheroids' diameters were about 500 µm when treatment with phlorizin occurred.

Resazurin, also known under the trade name Alamar Blue, is an active ingredient and cell viability indicator which represents a nontoxic and sensitive method in analysis of cell proliferation and cytotoxicity in various human and animal cell lines. For the following experiments a concentration of 0.11 mg resazurin dissolved in 1 ml DPBS was used. Then, 20 µL of the solution were added to each spheroid and incubated for 6 hours at 37°C under humidified atmosphere with 5% CO_2. After incubation, fluorescence was measured, whereat the wave length of excitation was approximately 540 nm and for emission it was 590 nm (figure 10). The principle behind this assay underlies the reducing power of living cells to irreversibly convert resazurin to resorufin, a fluorescent molecule. The amount of fluorescence is proportional to the number of living cells and corresponds to the metabolic activity of the cells. Damaged or even dead cells have lower metabolic activity and therefore generate a lower signal than viable cells. [50, 51]

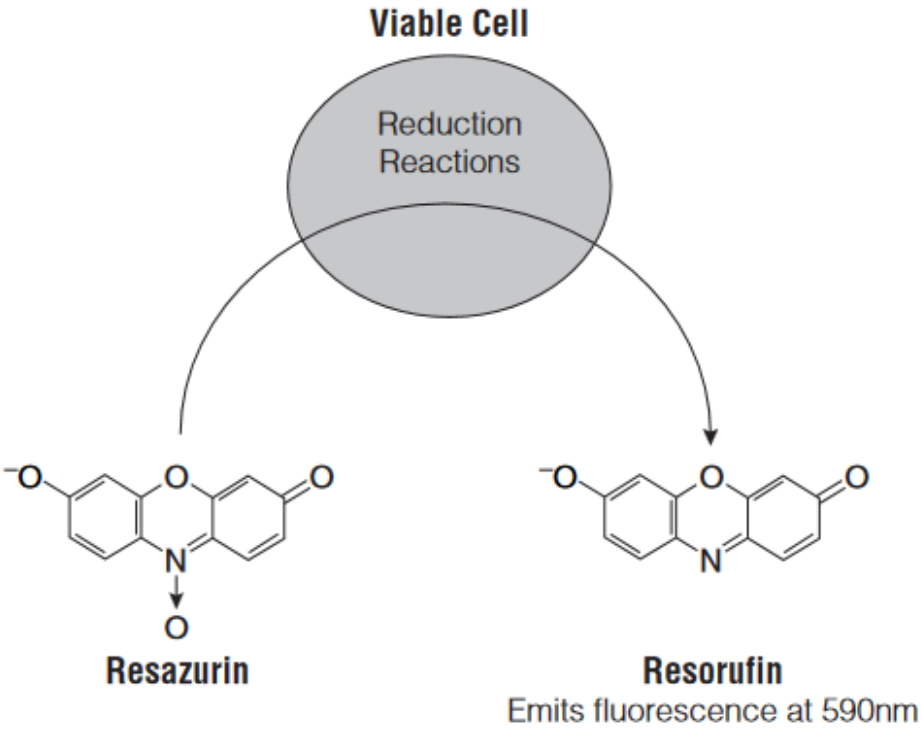

Figure 10: *As shown in the figure, the oxidized form resazurin is reduced to resorufin, which fluoresces at a wave length of 590 nm. (Source: Meck K. Etablierung von Frozen Instant Assays mit kryokonservierten Zellen in 384-Well-Platten für Hochdurchsatzscreenings. 2010; page 27)*

3.5 Treatment of multicellular tumor spheroids

3.5.1 Preparation of inhibitor

For each inhibitor three different concentrations (labelled from one for the highest to four as the lowest concentration) were applied, which were 50 µM, 5 µM and 0.5 µM in case of apigenin. For BCH, the highest concentration started with 5 mM, followed by 0.5 mM and 0.05 mM. After accomplishing the cell proliferation test for phlorizin, chosen concentrations were 1 mM, 0.1 mM and 0.01 mM. In addition, the fourth concentration consisted in growth media only, serving as negative control sample (figure 11).

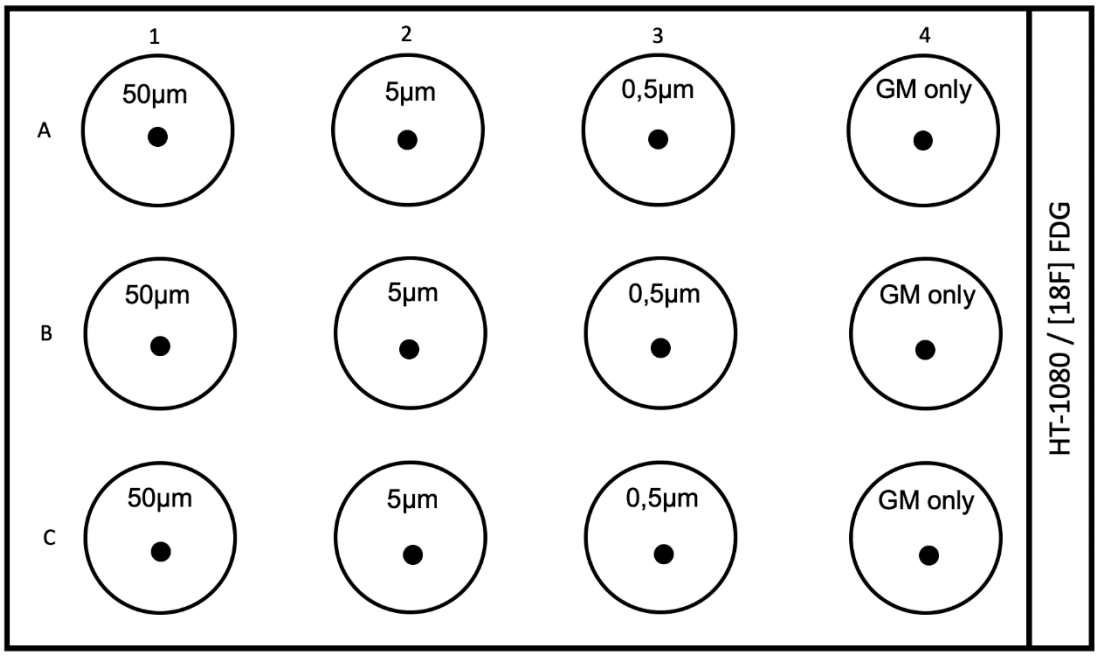

Figure 11: *This figure shows the preparation of different inhibitor concentrations in case of apigenin for cell line HT-1080, which afterwards is going to be treated with [^{18}F]FDG (GM: growth media)*

For making the inhibitor solution, a specific amount of substance was weighed in a Falcon^{TM} tube and the amount of substance n was calculated by using molecular weight (n=m/M). The volume of growth media in which the substance was supposed to be solved in was determined (V=n/c). In order to increase the inhibitor's solubility in growth media, 2% DMSO as organic solvent were added to the Falcon^{TM} tube. Again, the importance of complete solubility was put forward.

In the course of cell treatment, 100 µL of each concentration were pipetted to 96-well plates containing the previously selected triplicates of spheroids of the cell line which was supposed to be analyzed. Furthermore, incubation took place for 24 hours at 37°C under humidified atmosphere with 5% CO_2.

For radiotracer accumulation experiments, spheroids of all three cell lines were grown until they reached the desired diameter of 500 to 600 µm. Afterwards, the spheroids were treated with the respective inhibitors for 24 h. Then, [^{18}F]FDG, [^{18}F]FEC, [^{18}F]FET or [^{11}C]MET were added at 37°C for 50 min or 30 min, respectively. All experiments were performed in triplicates and repeated at least three times. Tracer uptake was calculated as

percentage of accumulated tracer in reference to the applied amount of radiotracer *via* measurement in the γ-counter.

3.5.2 Application and accumulation experiments of PET-tracers in treated multicellular tumor spheroids

At the end of the respective incubation time, all twelve treated spheroids were transferred to a flat bottomed, labelled 12-well plate and the size was measured under the microscope. A target concentration of 3 MBq of radioactivity per well, 500 µL respectively, was set for accumulation experiments. By measuring the tracer's radioactivity in a defined volume at a certain time, it was possible to calculate the amount of radioactive solution needed to reach a concentration of 39 MBq suspended in 6.5 mL growth media (6 MBq/mL). Afterwards, 500 µL of above-mentioned solution were added to each well containing one spheroid and incubated at 37°C under humidified atmosphere with 5% CO_2. Dependent on the used isotope, incubation time was 50 minutes in case of fluorine-18, and 30 minutes if experiments with carbon-11 were performed.

Subsequently, test samples for gamma counter measurement were prepared using Eppendorf vials. Therefore, 20 µL of the stock solution were transferred into three vials measured in triplicates as reference measurement. Then, all media containing radioactivity was removed – except for the spheroids. At this point it was important to work fast in order to reduce local body exposure, but also to pay attention to not losing a spheroid. After that, all spheroids were washed three times with 500 µL of DPBS, leaving the last liquid level. Again, 20 µL of the liquid of the last washing step were transferred into vials for background measurement in order to determine the amount of residual radioactivity. For accumulation measurement in spheroids, 100 µL of all concentrations were pipetted into three vials each – including the spheroids this time. In order to have the same amount of liquid (in this case 20 µL) in all cuvettes, 80 µL of liquid only were removed from all twelve cuvettes containing spheroids. Now, samples were ready for measurement in the gamma counter.

The results were calculated as follows:

$$\frac{(sample - blank)}{reference} * 100$$

Equation 1

Values for sample, blank and reference were decay corrected.

Sample measurement and statistical analysis:

For measurement of the radioactive samples, a well calibrated γ-counter (Wizard 2, PerkinElmer, Massachusetts, United States) was used.

All results are depicted as mean ± standard deviation and calculated with MS Excel, if not stated otherwise. Results were normalized to the control sample.

Normalization takes place *via* the following formula:

$$\frac{value\ of\ treated\ spheroid}{value\ of\ control\ spheroid}$$

Equation 2

Analysis for statistical significance was performed by GraphPad Prism by applying a one-way ANOVA calculation.

3.6 PET-tracer synthesis

All PET tracers were produced at the Department of Biomedical Imaging and Image-guided therapy of the General Hospital (AKH) in Vienna, Austria.

4 Results

4.1 Spheroids formation and growth behavior

The multicellular tumor spheroids of all three cell lines, which were formed by cultivating cell suspensions in 96-well plates coated with 1.5% agarose, showed variable morphology (figure 12). In general, spheroids were more dense for HT-29 and HCT-116 as for HT-1080 cells, which potentially reflect the cells origin. Both cells, HT-29 and HCT-116 cells are colon-carcinoma cell lines, whereas HT-1080 cells are a fibrosarcoma cell line.

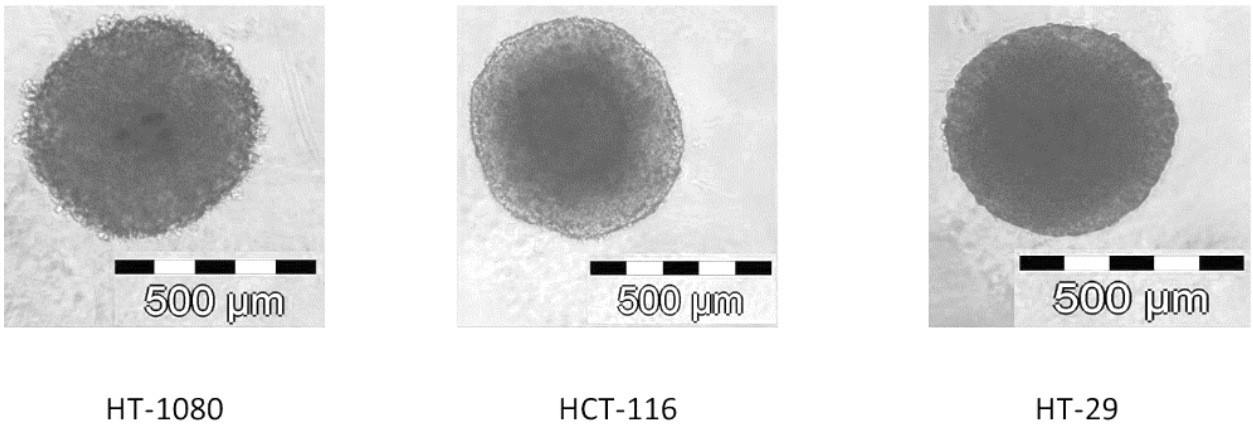

Figure 12: *Diverse morphology of the spheroids of cell line HT-1080, HCT-116 and HT-29*

It took about one week for spheroids of cell line HT-29 to reach a diameter between 500 µm and 600 µm, whilst spheroids of cell lines HCT-116 and HT-1080 with equal dimension were already formed after approximately three days, accounting the different seeded cell number. Hence, treatment with inhibitors was performed three days after seeding cells of HT-1080 and HCT-116, whereas spheroids of cell line HT-29 were treated seven days after seeding, in order to treat spheroids of similar size.

In conclusion, the cultivation in round 96-well plates of spheroids was highly reproducible and fast leading to spheroids uniform in shape and size without any supplements, like gelatin, agarose or Matrigel®.

4.2 Characterization of multicellular tumor spheroids

In order to investigate if the spheroids form a necrotic chore, spheroids of different size were stained with Calcein AM (staining of living cells) and propidium iodide (staining of necrotic cells) (figure 13). A necrotic chore was found for spheroids of all investigated cell lines at a size of around 500 µm or bigger, indicating the formation of the complex tumor environment including a proliferating outer sphere, a necrotic inner sphere and an intermediate zone with mostly quiescent cells. In order to reflect the *in vivo* situation, only multicellular tumor spheroids with a necrotic chore were used for further experiments. Therefore, spheroids in a size range of 500-600 µm were chosen for accumulation experiment to mimic the tumor situation as closely as possible.

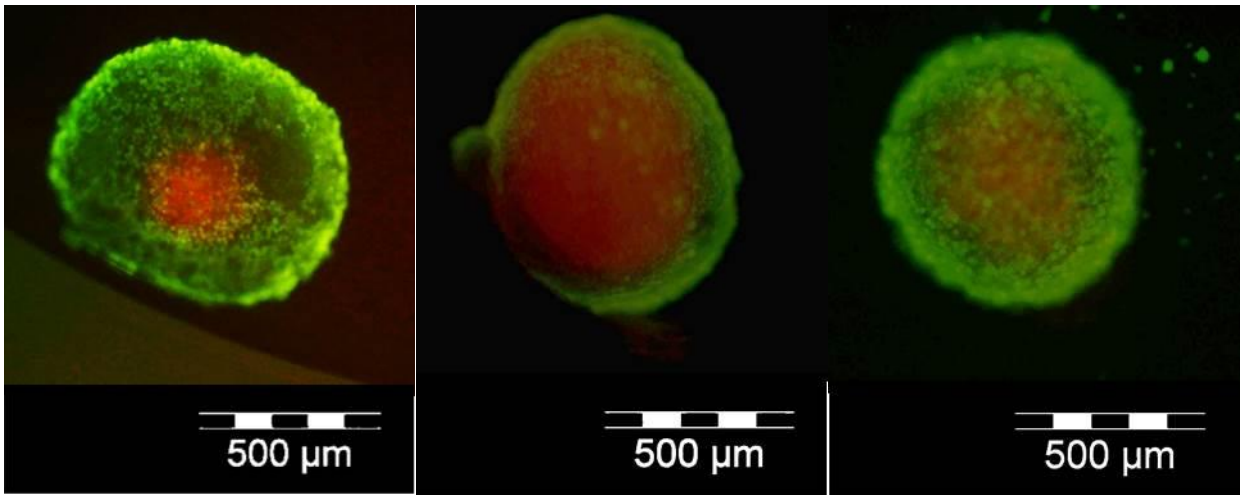

Figure 13: *Live-dead staining of HT-29, HCT-116 and HT-1080. Live cells appear as green, while necrotic cells appear as red*

4.3 Influence of phlorizin on proliferation of spheroids

Phlorizin was tested on its antiproliferative activity in spheroids by means of an Alamar Blue assay, in order to find a suitable concentration range of the inhibitor without inducing cell death. As necrosis or apoptosis would also reduce the active transport of cells and therefore would lead to misleading results. However, the IC_{50} of phlorizin was not reached in all three cell lines and therefore no antiproliferative effect was observable (figure 14). Due to the limitation of phlorizins' solubility higher concentrations were not possible. Consequently, no antiproliferative concentration is possible for phlorizin for the tested cell

lines. Therefore, the following concentrations were chosen for the upcoming accumulation experiments: 1 mM, 0.1 mM and 0.01 mM.

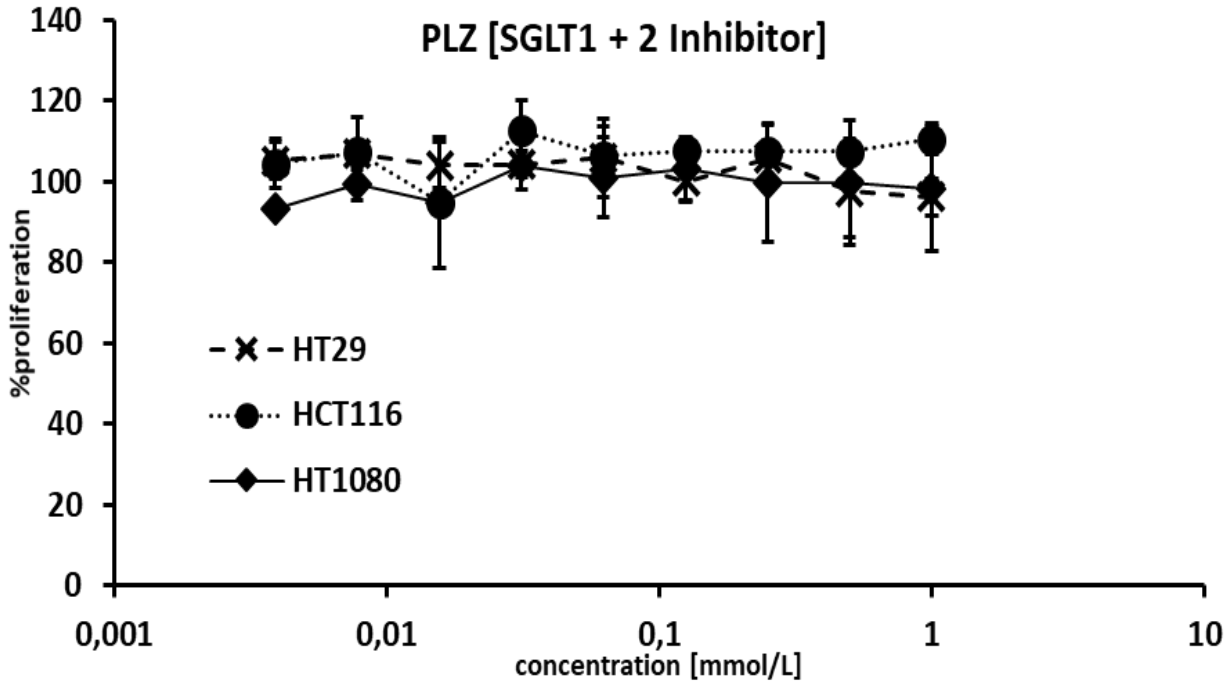

Figure 14: *IC_{50} for phlorizin was found to be higher than 1 mM and therefore not achievable, due to the limited solubility of this compound*

4.4 PET-tracer accumulation in treated multicellular tumor spheroids

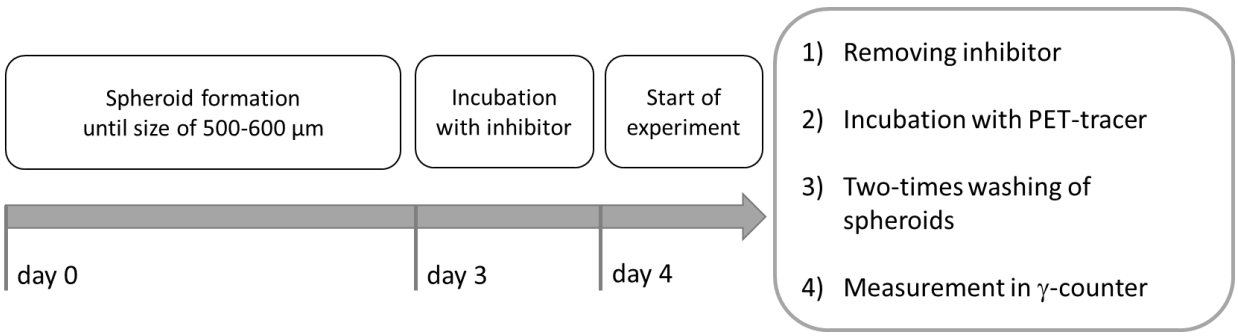

Figure 15*: Time schedule for performing PET-tracer accumulation*

In order to obtain replicable results, it was crucial to adhere strictly to the time schedule as shown in the figure above (figure 15). Since HT-29 spheroids require a few more days than cell line HT-1080 and HCT-116 to be formed, incubation with the inhibitor took place not until day 7, followed by removing the inhibitor one day later.

As soon as the spheroids reach a size of approximately 500-600 µm, they were treated with the respective inhibitor for 24 h. Afterwards the solution including the inhibitor was fully removed and fresh cell culture media including 3 MBq/mL of the PET-tracer were added. Therefore, potential effects are not generated by competitive inhibition, as the inhibitor was removed in advance. Only inhibitory effects, associated with non-competitive or uncompetitive inhibition should be visible.

4.4.1 Accumulation of [^{18}F]FDG

As noticeable by the figure below, [^{18}F]FDG was the only tracer used for accumulation experiments in all three cell lines, whereas only cell lines HCT-116 as well as HT-1080 were used in case of [^{18}F]FEC, [^{18}F]FET and [^{11}C]MET.

For all three cell lines, the accumulation for [^{18}F]FDG decreases in parallel to the applied concentration of the inhibitors apigenin and phlorizin as shown in the bar graph below (figure 16).

BCH only shows an intense effect in HCT-116 cells. In cell line HT-29 a significant impact was only observed at the highest concentration. However, in HT-1080 spheroids, the accumulation with [^{18}F]FDG showed no significance compared to non-treated cells.

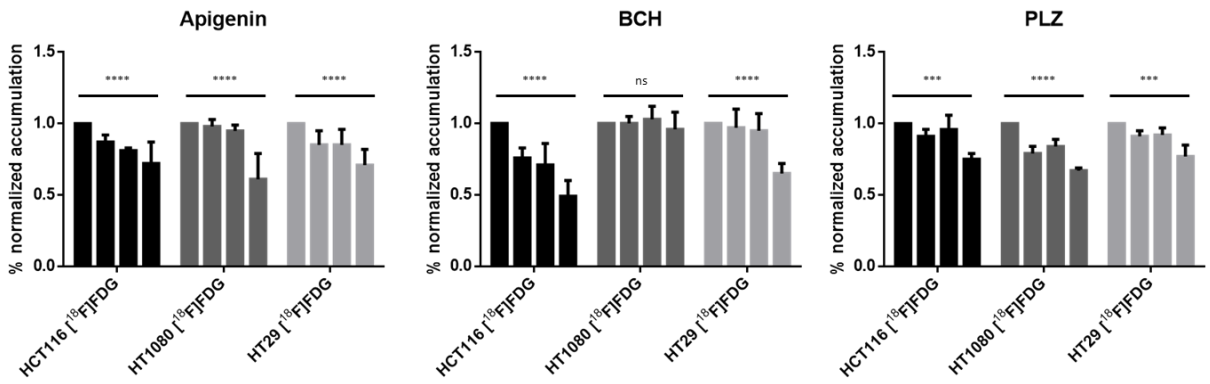

Figure 16: *Accumulation of [^{18}F]FDG in cell lines HCT-116, HT-1080, HT-29 treated with the respective inhibitors. Each bar on the left of every cell line represents the tracer accumulation measured in non-treated spheroids which was defined as 1%. The other three bars illustrate the accumulation in spheroids provided with the respective inhibitors, starting from the left with the lowest concentration to the right with the highest concentration*

4.4.2 Accumulation of [^{18}F]FEC

In case of apigenin, [^{18}F]FEC accumulation was not inhibited with the only exception of the highest apigenin concentration in both cell lines, which showed a minor reduction of [^{18}F]FEC accumulation of around 20% (figure 17A).

Also for BCH treatment, there was no influence on the accumulation of [^{18}F]FEC in both cell lines. Nevertheless, for phlorizin a difference was found for the used cell lines. In HCT-116 spheroids inhibited with phlorizin no effect was observed, whereas spheroids of cell line HT-1080 showed a significant reduced accumulation at the two highest concentrations.

4.4.3 Accumulation of [^{18}F]FET

Generally, apigenin and phlorizin affect the accumulation of [^{18}F]FET more than BCH does (figure 17B). In case of apigenin, spheroids of cell line HCT-116 showed significance in tracer accumulation at the two highest concentrations, whereas in HT-1080 spheroids, the inhibition had an impact only at the highest concentration.

For inhibition with phlorizin, nearly the same outcome could be observed as mentioned above in case of apigenin.

More precisely, BCH inhibition also showed an explicit significance only at the highest concentration in HCT-116 spheroids. However, in HT-1080 spheroids no effect compared to non-treated cells could be observed.

4.4.4 Accumulation of [^{11}C]MET

In conclusion, all inhibitor treatments led to a significant accumulation outcome, more precisely, the higher the concentration of the inhibitor was, the lower was the accumulation of [^{11}C]MET in spheroids (figure 17C).

A

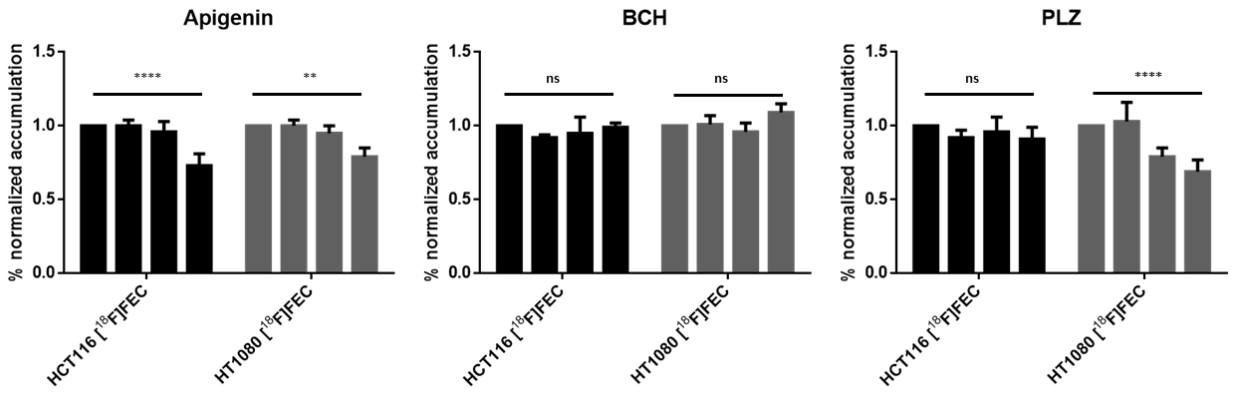

B

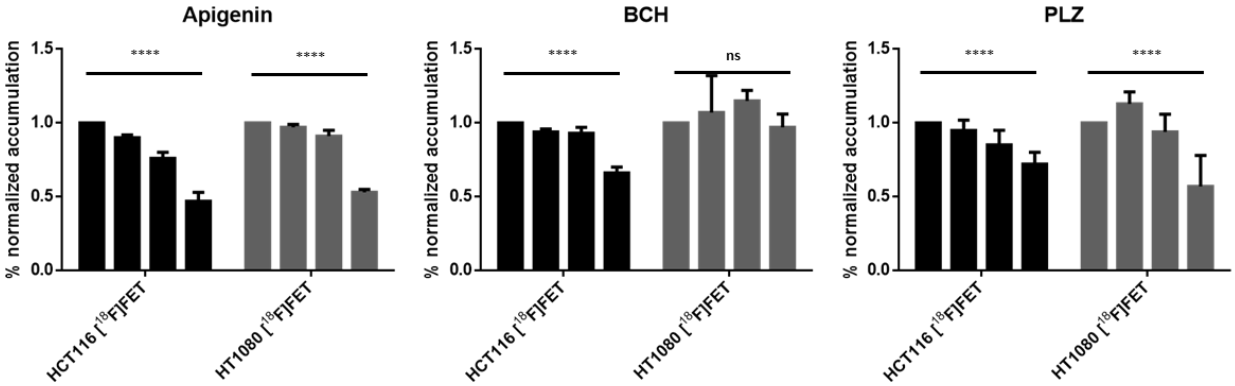

C

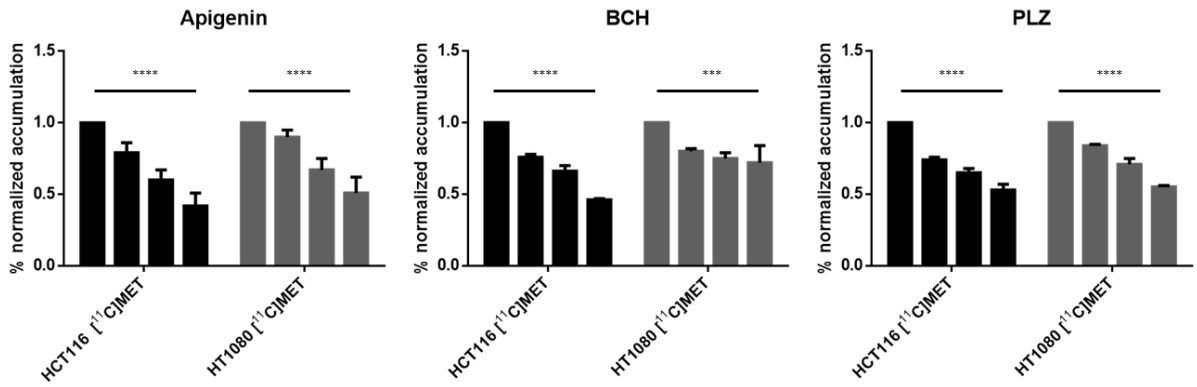

Figure 17: *Accumulation of (A) [^{18}F]FEC, (B) [^{18}F]FET and [^{11}C]MET in cell lines HCT-116 and HT-1080 treated with the respective inhibitors*

5 Discussion

5.1 Spheroids formation and growth behavior

Spheroids successfully imitate human tumor tissues and therefore are often used for different assays in oncology. However, only a minor amount of publications are present for the preclinical investigation of PET-tracers for oncological issues.

Compared to the hanging drop method, the formation of spheroids in agarose coated round-bottom plates was more reproducible and constant. This was important due to the precise time schedule of the planned experiments and the organization of the PET-tracer availability.

5.2 Characterization of multicellular tumor spheroids

Despite the fact that 2D cell monolayers have several limitations and are not fully able to reflect the functional behavior of cells found *in vivo*, they are often used for *in vitro* experiments. Since cultivation is conducted in a flask, they are forced into a monolayer morphology, which subsequently leads to a lack of cell-cell interactions as well as cell-matrix interactions. Moreover, molecular gradients and their impact on the metabolism of the cells are disregarded in 2D tumor cell monolayers.

In contrast, these missing features can be found in multicellular tumor spheroids, which therefore allows for a closer simulation of real tumor tissue. Their increase in size goes along with the appearance of molecular gradients, which results in the formation of a penetration barrier for drugs, metabolites, oxygen and other nutrients. [7] Furthermore, spheroids possess selective gates such as tight junctions which consist of transmembrane as well as cytoplasmic proteins like occludin and claudin to only name a few. Their main function is to regulate cellular diffusion of solutes and ions in order to guarantee sealing and form selective channels for material transport. This transport across an epithelial cell layer may be either a passive paracellular or a transcellular pathway, which is receptor mediated. [52-54]

Hence, connection between tight junctions allow for communication between cells and with their surrounding neighborhood. In 2D cell monolayers, these cell-cell interactions are

more or less represented by cell-to-plastic interactions, which do not provide the possibility of mimicking the *in vivo* environment of real tumor tissue.

In conclusion, multicellular tumor spheroids more closely represent the *in vivo* environment of real tumors in comparison to 2D cell monolayers.

5.3 Influence of phlorizin on proliferation of spheroids

As mentioned before, none of the tested phlorizin concentrations had a negative impact on the proliferation of spheroids. Concentrations of phlorizin used in past experiments and published in literature often ranged between 0.037 µM and 100 µM and did not show any toxic effects on the cells. [55-57]

5.4 PET-tracer accumulation in treated multicellular tumor spheroids

Accumulation of sugars, amino acids and other small molecular-weight compounds is very well described in literature for 2D cell culture. However, it is more difficult to analyze the more complex situation in 3D cell culture, as the transportation process consists of a set of serial or parallel events to enable accumulation in spheroids. These events consists of intracellular accumulation mechanism on the outer layer of the spheroid, whereas for the inner layers first a paracellular transport or diffusion has to occur, before an intracellular accumulation can take place. This complexity is furthermore increased by the fact, that small molecular-weight compounds are rarely selective compounds targeting only one transporter or receptor, but mostly lead to a set of different effects.

Therefore, these additional effects have to be considered when analyzing the results of the accumulation experiments.

In case of [^{18}F]FDG, the decreasing accumulation was expectable for GLUT1 and SGLT1/2 inhibitors, since this tracer is taken up by glucose transporters to find itself trapped intracellularly after phosphorylation. Studies have shown before the inhibitory effect of pretreatment with phlorizin on its substrates which in this case were fluoro-18-labelled glucosides. [58] Therefore, a decrease in tracer uptake was expected in case of glucose derivative [^{18}F]FDG.

According to results of a study, undifferentiated cells did not show a sodium-dependent accumulation of the sugar analogue methyl alpha-D-glucoside. In order to illustrate the expression of SGLT and its modulation by glucose, differentiated HT-29 cells grown in medium free of glucose were switched to a glucose containing medium. In that condition the sodium-dependent uptake of the sugar analogue was almost abolished. Nevertheless, when these cells were switched back to glucose-free medium, the uptake was restored again, although at a much lower level. These findings demonstrate the suitability of cell line HT-29 to study the regulation of the sodium-dependent glucose transporter. (59)

In the course of another study, evidence was provided for the assumption that the system of SGLT is a multimeric structure, in which the responsibility for phlorizin binding is attributed to certain complexes. (60) In order to emphasize these results, brush-border membranes of calf kidney cortex expressing SGLT, which were irradiated, were used. Afterwards, it was shown that a subsequent inactivation of phlorizin binding was due to a decrease in the number of high-affinity phlorizin binding sites rather than in their affinity itself, which underlines the correlation between SGLT and phlorizin.

Rather astonishing was the reduction of tracer accumulation by inhibiting LAT1 with BCH, taking into account that [^{18}F]FDG should not be transported by any amino acid transporter. More precisely, a reduction of accumulation could only be observed in spheroids of HT-29 and HCT116. This fact underlines the assumption, that the origin of cellular tissue may play a role in accumulation of PET-tracers in spheroids, since both cell lines derive from colon cancer.

Another possible reason for the observed effect may also lay in an altered metabolism of the cell. For example, studies have shown that an increase in [^{18}F]FDG uptake observed in thyroid carcinoma cell line ML-1 is no longer mediated by GLUT1, which may reflect activation of intracellular signal transduction cascades by oncogenes. (61) This leads to the assumption that [^{18}F]FDG accumulation might also depend on other transport systems than exclusively GLUT1, which have been affected by the inhibition of LAT1. This could be an explanation, why an inhibitory effect was observed in two cell lines in case of BCH.

In consideration of the tracer [^{18}F]FEC, inhibiting LAT1 did not have a significant effect on the accumulation as expected before. When looking at the obtained results in terms of tracer accumulation after inhibition with BCH, it is noticeable, that the impact of its inhibito-

ry effect is rather poor. In contrast, GLUT1 as well as SGLT1/2 inhibition had an unforeseeable impact on the tracer's accumulation in the spheroids. Moreover, SGLT1/2 inhibition showed an effect in spheroids of fibrosarcoma cell line HT-1080 only. The distinctive inhibitory effect of these two substances could be observed in all tracers used during the performed experiments.

Unexpected accumulation outcomes may be attributed to a change in appearance of choline kinase as its activity normally is elevated in neoplasms. [62] Nevertheless, a possible reason could lay in the consequences which inhibiting GLUT1 and SGLT1/2 had on the tumor spheroids. Due to a subsequent altered cell metabolism which might go along with decreased activity of choline kinase the accumulation of [^{18}F]FEC tended to be also inhibited by apigenin and phlorizin.

LAT is a major nutrient transport system responsible for the transport of amino acids which plays a critical role in cell growth and proliferation. Generally, LAT1 isoform is the major transporter of tyrosine in human fibroblast cells. Previous studies have shown that LAT1 is highly expressed in various human neoplasms, which often goes along with a poor prognosis in various human cancers. As an amino acid derivative, [^{18}F]FET as well is transported by amino acid transporters like LAT1. Nevertheless, BCH showed an effect only in cell line HCT-116, whereas no inhibition could be observed in spheroids of fibrosarcoma cell line HT-1080 contrary to expectations, which is rather astonishing due to the fact that LAT1 acts as the major transporter of tyrosine in fibroblasts. [63] Still, the absence of primarily expected decrease in tracer accumulation in cell line HT-1080 could be explained by the slowly reversible inhibitory effect of BCH.

According to another study, BCH as a very small compound was transported at very high rate into cells, which led to the opinion, that BCH acts more like a substrate of LAT1 than as an inhibitor. This might also explain why in many studies the uptake of L-leucine as well as cell growth have been reduced only at a very high concentration of BCH. [34] Furthermore, the fact, that the inhibitor was removed from the spheroids right before incubation with the tracer took place should be taken into account.

Although human fibroblast cells are an advantageous model to study the transport of amino acids across cell membranes, a major problem in many earlier studies is the lack of detailed knowledge regarding the expression and functionality of tyrosine transporters in

human fibroblasts. In the following study, a systematic functional characterization of the tyrosine transport in healthy fibroblasts with respect to the isoforms of system-L (LAT1-LAT4) was created. Therefore, uptake of L-tyrosine in fibroblasts was measured using various inhibitors. It was demonstrated that LAT1 was involved in 90% of total uptake of tyrosine. Not more than 10% could be accounted for by LAT2, LAT3 and LAT4 isoforms. LAT2 seemed to be functionally weak in uptake of tyrosine while LAT3 and LAT4 contributed around 7%. 10% could be contributed by system-A (ATA2 isoform). This finding raises the question, if tyrosine uptake in cells with inhibited LAT1 is switched to another isoform of the L-system such as LAT3, LAT4 or system-A. Additionally, competition between tyrosine and alanine for transport is shown to exist, probably between LAT1 and LAT2 isoforms. [64]

Another assumption lays in the fact that LAT1 requires 4F2hc (SLC3A2) cell surface antigen CD98 for its functional expression on the plasma membrane. In Western blot assays with T24 human bladder carcinoma cells, hLAT1 and h4F2hc have been confirmed to be linked to each other *via* a disulfide bond. Moreover, the subserving system LAT1 found in C6 rat glioma cells requires 4F2 heavy chain for its functional expression. As studies have shown the function of this complex is based on providing cells with essential amino acids for cell growth and cellular responses. When expressed in Xenopus oocytes with human 4F2hc, LAT1 tends to transport large neutral amino acids with high affinity as well as L-glutamine and L-asparagine with low affinity. It was proven that while all tumor cell lines examined in the study express hLAT, the expression of h4F2hc is varied particularly in leukemia cell lines. [65] This leads to the assumption that possible lack of h4F2hc expression in further cell lines like HT-1080 results in absence of LAT1 and therefore, BCH did affect neither the amino acid transport system nor [^{18}F]FET accumulation.

Furthermore, LAT1 provides cancer cells with essential amino acids not only for protein synthesis, but also for stimulation of growth of cancer cells *via* mammalian target of rapamycin mTOR. Recently, Yamauchi *et al*. reported that an inhibitor of system L-amino acid transporter reduced the level of phosphorylation of mTOR and its downstream signaling molecules in a head and neck squamous cell carcinoma cell line. [66] Subsequently, this leads to decrease in cell proliferation as well as down-regulation in cell metabolism, which might have also happened in case of inhibition with BCH in cell line HT-1080.

As noticed, GLUT1 as well as SGLT1/2 inhibition again had an unpredictable effect on the spheroids.

For [^{11}C]MET, all three inhibitors had a noticeable impact on the tracer's accumulation in the spheroids, although it only was predictable due to studies in case of BCH.

A recent study elucidated the transport mechanisms of [^{11}C]MET in normal human astrocytes, low-grade as well as high-grade human glioma cell lines. Because of the short half-life of carbon-11, [^{14}C]MET was used instead of the PET tracer for *in vitro* experiments. Results showed that the uptake of [^{14}C]MET was inhibited strongly by BCH, which demonstrates that the L-system is predominantly involved in transport of [^{11}C]MET in glioma cells and human astrocytes. [67, 68] In another study the usefulness of [^{11}C]MET as tracer for staging myeloma cells with highly expressed LAT1 on their surfaces was supported. [69]

As already known for thyrosine, L-type amino acid transporter 1 is essential for the transport of large neutral amino acids like methionine too. For its functional expression, LAT1 requires the heavy chain of 4F2 cell surface antigen like described above. The aim of the following study was to elucidate the correlation of LAT1 and 4F2hc expression with [^{11}C]MET uptake in patients recently diagnosed with human gliomas. In conclusion, the expression of LAT1 and 4F2hc was much higher in high-grade gliomas than in low-grade gliomas and the expression of LAT1, but not 4F2hc was significantly correlated with [^{11}C]MET uptake. [70]

Based on all these results, a decrease in tracer accumulation could be expected in case of BCH.

As mentioned before, it often is difficult to distinguish passive diffusion from carrier-mediated transport, that both are attributed to a majority of drug transport. Based on the knowledge, that the latter can be saturated at excess of substrate concentrations, it might be assumed that passive diffusion plays an important role, if the accumulation of a drug is not saturable. However, besides above mentioned passive transport mechanism, energy-dependent processes like membrane trafficking and endocytosis regulating the exchange of molecules in between the organelles mostly mediated by vesicles could also contribute to a concentration-independent accumulation of small molecules. In assays, the relative role of carrier-mediated drug transport was revealed by analysing the relative uptake between an empty vector transfected cells and cells overexpressing transporters. Unfortu-

nately, it is not yet possible to determine the task significance of drug transport by passive diffusion *in vivo* at the moment. On the contrary, it may be possible to determine the significance of a transporter or family of transporters in intracellular drug uptake experiments. While passive diffusion or yet unknown transporters could be conducive to drug uptake, several other mechanisms like membrane trafficking could also be of paramount importance. Nevertheless, its relevance in contributing to drug transport still remains underappreciated. [23]

6 Conclusion

The aim of this diploma thesis consisted in the evaluation of the accumulation of PET-tracers in multicellular tumor spheroids, cultivated out of various cancer cell lines and treated with different inhibitors.

In order to obtain spheroids which were uniform in shape and size, the cultivation in previously with agarose coated 96-well plates turned out to be highly reproducible as well as fast method for all tested cell lines, although HT-29 cells needed longer to build dense cell aggregates than cell lines HCT-116 and HT-1080.

Additionally, by performing cell viability assays, it could be confirmed that the increase of necrotic cells within multicellular tumor spheroids goes along with the size of the spheroid. Spheroids bigger than 500 µm already manifested a necrotic core.

Considering the outcome of the phlorizin toxicity assay, it could be concluded that none of the used concentrations had a negative impact on the cells. Therefore, concentrations of 1 mM, 0.1 mM and 0.01 mM were applied to the spheroids after reaching a size of approximately 500 µm.

By conducting *in vitro* experiments using 3D cell aggregates it was possible to evaluate the accumulation outcome for each tested radiotracer as well as cell line. On the one hand, PET-tracer accumulation experiments turned out as anticipated, on the other hand, it could be revealed that inhibitors, which were expected to have or rather not have an impact on the accumulation in the spheroids caused quite the opposite event. Noticeable was the distinct, often not predictable inhibitory effect of apigenin as well as phlorizin. Moreover, it seemed like the origin of the cellular tissue had an impact on whether the inhibitors affected the tracer accumulation or not. Furthermore, an altered cell metabolism – like receptor up/down regulation or non-competitive inhibition – induced by the inhibitors themselves, could be a possible explanation for unforeseen accumulation results.

Summarized it can be said that due to the similarity to human tumor tissue, multicellular tumor spheroids could replace 2D cell monolayers in preclinical PET-tracer evaluation assays. Additionally, their application could lead to savings of animal experiments in the fu-

ture due to their capability of closing the gap of needed information between 2D cell cultures and animal experiments.

7 Abbreviations

API	Apigenin
DPBS	Dulbecco's Phosphate-Buffered Saline
FBS	Fetal bovine serum
[^{18}F]FDG	2-Deoxy-2-[^{18}F]fluoroglucose
[^{18}F]FEC	2-[^{18}F]fluoroethyl-choline
[^{18}F]FET	O-(2-[^{18}F]fluoroethyl)-L-tyrosine
GLUT1	Glucose transporter 1
LAF	Laminar air flow
LAT1	Large neutral amino acid transporter
MEM	Minimum essential medium
[^{11}C]MET	L-[methyl-^{11}C]methionine
MTS	Multicellular tumor spheroids
PET	Positron emission tomography
PLZ	Phlorizin
SGLT1/2	Sodium dependent glucose cotransporter 1/2

8 Equation list

9 References

1. Holtfreter J. A study of the mechanism of gastrulation. Journal of Experimental Zoology. 1944;95:171–212.
2. Sutherland RM, Durand RE. Growth and cellular characteristics of multicell spheroids. Recent Results Cancer Res. 1984;95:24–49.
3. Freyer JP, Sutherland R. Regulation of growth saturation and development of necrosis in EMT6/Ro multicellular spheroids by the glucose and oxygen supply. Cancer Research.1986;46 (7):3504–3512.
4. Mueller-Klieser W, Freyer JP, Sutherland RM. Influence of glucose and oxygen supply conditions on the oxygenation of multicellular spheroids. British Journal of Cancer.1986;53:345–353.
5. Casciari J, Sotirchos S, Sutherland R. Variation in tumor growth rates and metabolism with oxygen concentration, glucose concentration, and extracellular pH. Journal of Cellular Physiology.1992;151:386–394.
6. Hirschhaeuser F, Menne H, Dittfeld C, West J, Mueller-Klieser W, Kunz-Schughart LA. Multicellular tumor spheroids: an underestimated tool is catching up again. J Biotechnol. 2010;148:3–15.
7. Achilli TM, Meyer J, Morgan JR. Advances in the formation, use and understanding of multi-cellular spheroids. Expert opinion on biological therapy. 2012;12:1347-1360.
8. Benton G, Arnaoutova I, George J, Kleinman HK, Koblinski J. Matrigel: From discovery and ECM mimicry to assays and models for cancer research. Adv Drug Deliv Rev. 2014;15:79-80.
9. Schreiber-Brynzak E, Klapproth E, Unger C, Lichtscheidl-Schultz I, Goschl S, Schweighofer S, Trondl R, Dolznig H, Jakupec MA, Keppler BK. Three-dimensional and co-culture models for preclinical evaluation of metal-based anticancer drugs. Invest New Drugs. 2015;33:835-847.
10. Yamada KM, Clark K. Cell biologoy: Survival in three dimensions. Nature. 2002;419:790-791.
11. Jacks T, Weinberg RA. Taking the Study of Cancer Cell Survival to a New Dimension. Cell. 2002;111:923-925.

12. Santini MT, Rainaldi G. Three-dimensional spheroid model in tumor biology. Pathobiology. 1999;67:148–157.
13. McMahon KM, Volpato M, Chi HY, Musiwaro P, Poterlowicz K, Peng Y, Scally AJ, Patterson LH, Phillips RM, Sutton CW. Characterization of Changes in the Proteome in Different Regions of 3D Multicell Tumor Spheroids. J Proteome Res. 2012;11:2863–2875.
14. Franko AJ, Sutherland RM. Oxygen diffusion distance and development of necrosis in multicell spheroids. Radiat Res. 1979;79:439-453.
15. Sutherland RM. Cell and environment interactions in tumor microregions: The multicellular spheroid model. Science. 1988;240:177-184.
16. Sutherland RM, Durand RE. Radiation response of multicell spheroids—an in vitro tumour model. Curr Top Radiat Res Q. 1976;11:87–139.
17. Sutherland RM. Spheroids in Cancer Research. Cancer Res. 1981;41:2980-2984.
18. Mueller-Klieser W. Three-dimensional cell cultures: from molecular mechanisms to clinical applications. Am J Physiol. 1997;273:1109–1123.
19. Sutherland RM, Robson MacDonald H, Howell RL. A New Model Target for In Vitro Studies of Immunity to Solid Tumor Allografts: Brief Communication. Nati Cancer Inst. 1977;58:1849-1852.
20. Gambhir SS. Molecular imaging of cancer with positron emission tomography. Nature. 2002;2:683-693.
21. Qian Y, Wang X, Chen X. Inhibitors of glucose transport and glycolysis as novel anticancer therapeutics. World J Transl Med. 2014;3:37-57.
22. http://what-when-how.com/human-drug-metabolism/mechanisms-of-inhibition-cytochrome-p450-inhibition-human-drug-metabolism-part-1/
23. Cocucci, E., Kim, J., Bai, Y., Pabla, N. Role of Passive Diffusion, Transporters, and Membrane Trafficking-Mediated Processes in Cellular Drug Transport. Clinical Pharmacology & Therapeutics.2016;101(1):121–129.
24. Conde A, Diallinas G, Chaumont F, Chaves M, Gerós H. Transporters, channels, or simple diffusion? Dogmas, atypical roles and complexity in transport systems. 2010;42(6):857-68.

25. Melstrom LG, Salabat MR, Ding XZ, Milam BM, Strouch M, Pelling JC, Bentrem DJ. Apigenin inhibits the GLUT-1 glucose transporter and the phosphoinositide 3-kinase/Akt pathway in human pancreatic cancer cells. 2008;37:426-431.
26. Xu YY, Wu TT, Zhou SH, Bao YY, Wang Q, Fan J, Huang YP. Apigenin suppresses GLUT-1 and p-AKT expression to enhance the chemosensitivity to cisplatin of laryngeal carcinoma Hep-2 cells: an in vitro study. Int J Clin Exp Pathol. 2014;7:3938–3947.
27. Bao YY, Zhou SH, Lu ZJ, Fan J, Huang YP. Inhibiting GLUT-1 expression and PI3K/Akt signaling using apigenin improves the radiosensitivity of laryngeal carcinoma in vivo. Oncol Rep. 2015;34(4):1805-1814.
28. https://pubchem.ncbi.nlm.nih.gov/compound/5280443#section=InChI-Key. Downloaded on 28.01.2019
29. Napolitano L., Galluccio M., Scalise M., Parravicini C., Palazzolo L., Eberini I, Indiveri C. Novel insights into the transport mechanism of the human amino acid transporter LAT1 (SLC7A5). Probing critical residues for substrate translocation. Biochimica et Biophysica Acta (BBA) - General Subjects, 2017;1861(4), 727–736.
30. Scalise M, Galluccio M, Console L, Pochini L, Indiveri C. The Human SLC7A5 (LAT1): The Intriguing Histidine/Large Neutral Amino Acid Transporter and Its Relevance to Human Health. Front Chem. 2018;6:243.
31. Altan B, Kaira K, Watanabe A, Kubo N, Bao P, Dolgormaa G, Bilguun EO, Araki K, Kanai Y, Yokobori T, Oyama T, Nishiyama M, Kuwano H, Shirabe K. Relationship between LAT1 expression and resistance to chemotherapy in pancreatic ductal adenocarcinoma. 2018;81(1):141–153.
32. https://www.caymanchem.com/product/15249. Downloaded on 28.01.2019
33. Kim CS, Cho SH, Chun HS, Lee SY, Endou H, Kanai Y, Kim DK. BCH, an inhibitor of system L amino acid transporters, induces apoptosis in cancer cells. Biol Pharm Bull. 2008;31(6):1096-1100.
34. Huttunen KM, Gynther M, Huttunen J, Puris E, Spicer JA, Denny WA. A Selective and Slowly Reversible Inhibitor of l-Type Amino Acid Transporter 1 (LAT1) Potentiates Antiproliferative Drug Efficacy in Cancer Cells. 2016;59(12):5740-5751.
35. Imai H, Kaira K, Oriuchi N, Shimizu K, Tominaga H, Yanagitani N, Sunaga N, Ishizuka T, Nagamori S, Promchan K, Nakajima T, Yamamoto N, Mori M, Kanai Y. In-

hibition of L-type Amino Acid Transporter 1 Has Anti tumor Activity in Non-small Cell Lung Cancer. International Journal of Cancer Research and Treatment. 2010; 30(12):4819-4828.

36. Yothaisong S, Dokduang H, Anzai N, Hayashi K, Namwat N, Yongvanit P, Sangkhamanon S, Jutabha P, Endou H, Loilome W. Inhibition of l-type amino acid transporter 1 activity as a new therapeutic target for cholangiocarcinoma treatment. 2017; 39(3):1010428317694545.
37. https://pubchem.ncbi.nlm.nih.gov/compound/115288#section=Top
38. Blaschek W. Natural Products as Lead Compounds for Sodium Glucose Cotransporter (SGLT) Inhibitors. 2017;83(12-13):985-993.
39. https://pubchem.ncbi.nlm.nih.gov/compound/6072#section=Top
40. F Rosenwasser RF, Sultan S, Sutton D, Choksi R, Epstein BJ. SGLT-2 inhibitors and their potential in the treatment of diabetes. Diabetes Metab Syndr Obes. 2013;6:453–467.
41. Nagata T, Suzuki M, Fukazawa M, Honda K, Yamane M, Yoshida A, Azabu H, Kitamura H, Toyota N, Suzuki Y, Kawabe Y. Competitive inhibition of SGLT2 by tofogliflozin or phlorizin induces urinary glucose excretion through extending splay in cynomolgus monkeys. Am J Physiol Renal Physiol. 2014;306(12):1520-1533.
42. Malhotra A, Kudyar S, Gupta AK, Kudyar RP, Malhotra P. Sodium glucose cotransporter inhibitors – A new class of old drugs**.** Int J Appl Basic Med Res. 2015;5(3):161–163.
43. Som P, Atkins HL, Bandoypadhyay D, Fowler JS, MacGregor RR, Matsui K, Oster ZH, Sacker DF, Shiue CY, Turner H, Wan CN, Wolf AP, Zabinski SV. A fluorinated glucose analog, 2-fluoro-2-deoxy-D-glucose (F-18): nontoxic tracer for rapid tumor detection. J Nucl Med.1980;21:670-675.
44. Di Chiro G, de la Paz RL, Brooks RA, Sokoloff L, Kornblith PL, Smith BH, Patronas NJ, Kufta CV, Kessler RM, Johnston GS, Manning RG, Wolf AP. Glucose utilization of cerebral gliomas measured by [18F] fluorodeoxyglucose and positron emission tomography. Neurology. 1982;32:1323-1329.
45. Geinitz H, Roach M, van As N. Radiotherapy in Prostate Cancer: Innovative Techniques and Current Controversies. 2014.

46. Otabashi M, Vriamont C, Vergote T, Desfours C, Morelle JL, Philippart G. High yield [18F]FET production on AllinOne (Trasis) at commercial scale. URL: https://www.google.com/search?client=firefox-b-ab&q=High+yield+%5B18F%5DFET+production+on+AllinOne+%28Trasis%29+at+commercial+scale.+. Downloaded on 28.01.2019
47. Dunet V, Rossier C, Buck A, Stupp R, Prior JO. Performance of ^{18}F-Fluoro-Ethyl-Tyrosine (^{18}F-FET) PET for the Differential Diagnosis of Primary Brain Tumor: A Systematic Review and Metaanalysis. J Nucl Med. 2012;53(2):207-214.
48. Pauleit D, Stoffels G, Bachofner A, Floeth FW, Sabel M,Herzog H, Tellmann L, Jansen P, Reifenberger G, Hamacher K, Coenen HH, Langen KJ. Comparison of ^{18}F-FET and ^{18}F-FDG PET in brain tumors. Nucl Med Biol. 2009;36(7):779-787.
49. http://www.radiationanswers.org/radiation-introduction/detecting-measuring/gamma-counter.html. Downloaded on 13.01.2019
50. https://www.bio-rad-antibodies.com/alamarblue-cell-proliferation-assay.html. Downloaded on 13.01.2019
51. https://www.thermofisher.com/at/en/home/brands/molecular-probes/key-molecular-probes-products/alamarblue-rapid-and-accurate-cell-health-indicator.html. Downloaded on 13.01.2019
52. Zihni C, Mills C, Matter K, Balda MS. Tight junctions: from simple barriers to multifunctional molecular gates. Nat Rev Mol Cell Biol. 2016;17(9):564-80.
53. Aijaz S Balda MS, Matter K. Tight junctions: molecular architecture and function. Int Rev Cytol. 2006;248:261-98.
54. Rajasekaran SA, Beyenbach KW, Rajasekaran AK. Interactions of tight junctions with membrane channels and transporters. 2008;1778(3):757-769
55. Moran A, Davis LJ, Turner RJ. High affinity phlorizin binding to the LLC-PK1 cells exhibits a sodium:phlorizin stoichiometry of 2:1. J Biol Chem. 1988;263(1):187-92.
56. Kanda H, Kaneda T, Kawaguchia A, Sasaki N, Tajima T, Urakawa N, Shimizu K, Suzuki H. Phloridzin inhibits high K+-induced contraction via the inhibition of sodium: glucose cotransporter 1 in rat ileum. J Vet Med Sci. 2017;79(3): 593–601.
57. Nair SV, Ziaullah, Rupasinghe HP. Fatty acid esters of phloridzin induce apoptosis of human liver cancer cells through altered gene expression. PLoS One. 2014;9(9):e107149.

58. de Groot TJ, Veyhl M, Terwinghe C, Vanden Bempt V, Dupont P, Mortelmans L, Verbruggen AM, Bormans GM, Koepsell H. Synthesis of 18F-fluoroalkyl-beta-D-glucosides and their evaluation as tracers for sodium-dependent glucose transporters. J Nucl Med. 2003;44(12):1973-1981.
59. Blais A. Expression of Na(+)-coupled sugar transport in HT-29 cells: modulation by glucose. Am J Physiol. 1991;260:1245-1252.
60. Lin JT, Szwarc K, Kinne R, Jung CY. Structural state of the Na+/D-glucose cotransporter in calf kidney brush-border membranes. Target size analysis of Na+-dependent phlorizin binding and Na+-dependent D-glucose transport. Biochim Biophys Acta. 1984;777(2):201-208.
61. Prante O, Maschauer S, Fremont V, Reinfelder J, Stoehr R, Szkudlinski M, Weintraub B, Hartmann A, Kuwert T. Regulation of uptake of 18F-FDG by a follicular human thyroid cancer cell line with mutation-activated K-ras. J Nucl Med. 2009;50(8):1364-1370.
62. Kumar M, Arlauckas SP, Saksena S, Verma G, Ittyerah R, Pickup S, Popov AV, Delikatny EJ, Poptani H. Magnetic resonance spectroscopy for detection of choline kinase inhibition in the treatment of brain tumors. Mol Cancer Ther. 2015;14(4):899-908.
63. https://www.uniprot.org/uniprot/Q01650. Downloaded on 14.01.2019
64. Vumma R, Wiesel FA, Flyckt L, Bjerkenstedt L, Venizelos N. Functional characterization of tyrosine transport in fibroblast cells from healthy controls. Neurosci Lett. 2008;434(1):56-60.
65. Yanagida O, Kanai Y, Chairoungdua A, Kim DK, Segawa H, Nii T, Cha SH, Matsuo H, Fukushima J, Fukasawa Y, Tani Y, Taketani Y, Uchino H, Kim JY, Inatomi J, Okayasu I, Miyamoto K, Takeda E, Goya T, Endou H. Human L-type amino acid transporter 1 (LAT1): characterization of function and expression in tumor cell lines. Biochim Biophys Acta. 2001;1514(2):291-302.
66. Yamauchi K, Sakurai H, Kimura T, Wiriyasermkul P, Nagamori S, Kanai Y, Kohno N. System L amino acid transporter inhibitor enhances anti-tumor activity of cisplatin in a head and neck squamous cell carcinoma cell line. Cancer Lett. 2009;276(1):95-101.

67. Ono M, Oka S, Okudaira H, Schuster DM, Goodman MM, Kawai K, Shirakami Y. Comparative evaluation of transport mechanisms of trans-1-amino-3-[^{18}F]fluorocyclobutanecarboxylic acid and L-[methyl-^{11}C]methionine in human glioma cell lines. Brain Res. 2013;1535:24-37.
68. https://www.uniprot.org/uniprot/Q01650. Downloaded on 05.02.2019
69. Lapa C, Knop S, Schreder M, Rudelius M, Knott M, Jörg G, Samnick S, Herrmann K, Buck AK, Einsele H, Lückerath K. 11C-Methionine-PET in Multiple Myeloma: Correlation with Clinical Parameters and Bone Marrow Involvement. Theranostics. 2016;6(2):254-261.
70. Okubo S, Zhen HN, Kawai N, Nishiyama Y, Haba R, Tamiya T. Correlation of L-methyl-11C-methionine (MET) uptake with L-type amino acid transporter 1 in human gliomas. J Neurooncol. 2010;99(2):217-225.